High resolution sonography of peripheral nerves: normal values in healthy individuals and the role of sonography in rare disorders of peripheral nerves

PhD Thesis

Josef Böhm, MD

Semmelweis University

János Szentágothai Doctoral School of Neurosciences

Consultant: Dániel Bereczki, MD, DSc, professor

Referees:

Committee for PhD examination:
Chairman: István Bitter, MD, DSc, professor
Members: Anita Kamondi, MD, DSc, professor
Attila Valikovics, MD, PhD, chief neurologist

Budapest

2014

TABLE OF CONTENTS

ABBREVIATIONS

ADM	abductor digiti minimi muscle
APB	abductor pollicis brevis muscle
CSA	cross sectional area
CT	computer tomography
CTS	carpal tunnel syndrome
EDX	electrodiagnostic testing
EMG	electromyography
HRUS	high resolution ultrasound
MAP	muscle action potential
MRI	magnetic resonance imaging
NCAM	medial antebrachial cutaneous nerve
NCV	nerve conduction velocity
ONSD	optic nerve sheath diameter
PIN	posterior interosseous nerve
PTS	Parsonage-Turner syndrome
SD	standard deviation
SNAP	sensory nerve action potential
T	Tesla
TOS	thoracic outlet syndrome
UNE	ulnar neuropathy at the elbow
US	ultrasound

1. Introduction and background

1.1. Peripheral nerve imaging

Before the introduction of imaging methods the diagnostic work-up of peripheral nerve disorders was based only on evaluation of the clinical history, neurological examination and standard electrodiagnostic examination, consisting of nerve conduction studies, recording of late responses (F-waves) and needle electromyography (1). Nerve imaging became an important method in patient management by providing information on lesion morphology, anatomic location, relationship of lesions to surrounding soft tissue, and evaluation of areas difficult to access with electrodiagnostic methods. Imaging can also identify peripheral nerve lesions that are not apparent on electrodiagnostic testing. High resolution ultrasound (HRUS) and magnetic resonance imaging (MRI, MR-Neurography) are the most commonly used methods for visualizing peripheral nerves. Ultrasound (US) modified diagnostic and therapeutic management beyond the electrodiagnostic findings in as many as 43% of patients and had a confirmatory role in 40% of the patients. US complements neurophysiological assessment even in routine practice, and this confirms the increasing interest in US in a multidimensional evaluation of peripheral nervous system diseases (2). Types of peripheral nerve abnormalities suited for visualization by HRUS include changes in nerve caliber, continuity, echogenicity, echotexture, and vascularisation. Imaging can identify peripheral nerve tumours, traumatic lesions, entrapments with nerve damage, inflammation, demyelinating features, infections, and it can be used for imaging-guided interventions, such as nerve blocks, biopsies or therapeutic application of drugs. Intraoperative HRUS can show the extent of traumatic peripheral nerve lesions, it appears to be capable of assessing the type (intraneural/perineural) and grade of nerve fibrosis, and in combination with intraoperative neurophysiological studies it is an important tool for the non-invasive assessment of the regenerative potential of a nerve lesion (3).

HRUS and MRI are complementary methods, each having its advantages and disadvantages (4). For example, deep situated structures of the peripheral nervous system such as the lumbosacral plexus and the intrapelvic part of the sciatic nerve can be examined with much higher quality by MRI than with high resolution ultrasound.

Furthermore, MRI has a much higher contrast resolution, and contrast agents can be administered as well. However MRI is less available, time-consuming, and expensive, and normal values are hardly available. On the other hand, ultrasound has a higher spatial resolution, can be modified and tailored immediately to the pathology seen by the examiner, and it allows dynamic assessment.

1.2. High resolution ultrasound

High resolution sonography (HRUS) of peripheral nerves is a relatively new imaging field. First studies date back to the mid-1980s. In 1985, Solbiati et al. studied the recurrent laryngeal nerve by sonography (5), and Fornage published in 1988 the sonographic features of the median nerve in the carpal tunnel (6). However, with the previously available ultrasound equipment (Fornage used an Aloka device SSD-210 with 5-7.5 MHz linear array transducer, *Fig. 1*) only larger pathological nerve alterations could be detected.

Since then, all major manufacturers have improved the resolution and quality of their ultrasound images dramatically by means of high-frequency and high-resolution broad band linear array transducers up to 18 MHz, as well as by introduction of new image processing technologies. With these modern equipments, the number of publications in this field increase continuously, reaching more than 250 publications only the last year PubMed search for 2013 with the terms sonography and peripheral nerves. US can readily be used for the detection of nerve abnormalities caused by trauma, tumors, inflammation, and a variety of non-neoplastic conditions, including compressive neuropathies and polyneuropathies.

A

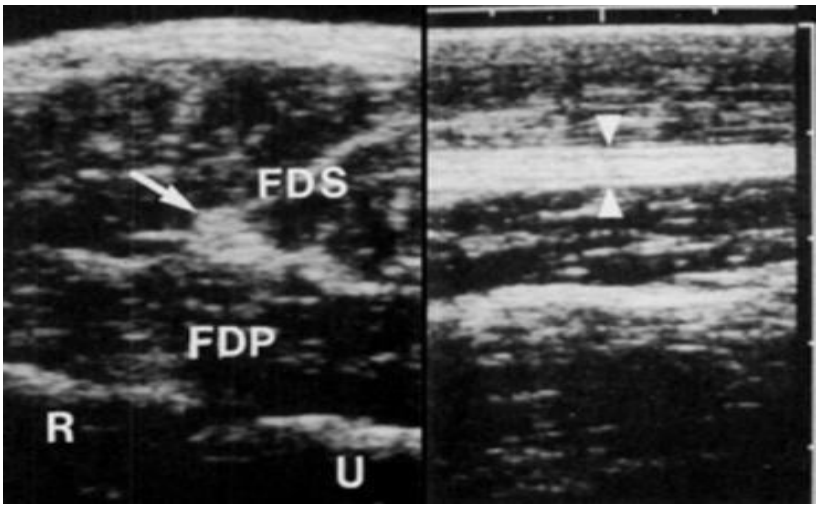

B

Figure 1. A. Aloka ultrasound device Echo Camera SSD- 210, 1983. (Reproduced from www.ob-ultrasound.net/manufacturers.html) **B**. US images of the median nerve on transverse and longitudinal scan (Fornage, 1988).

Advantages of the method, such as the possibility of dynamic examination, assessment of long nerves segments in a short time, bed-side-availability, non-invasivity and low cost, make US the ideal imaging tool in peripheral nerve disease (7).

In a retrospective study, the accuracy, sensitivity and specificity of MRI and US in the evaluation of mononeuropathies and brachial plexopathies was assessed in patients with focal peripheral nerve disease who had undergone both tests. Nerve

pathology was diagnosed in 47/53 patients, with US detecting abnormalities in 93% and MRI detecting only 67%. It was therefore concluded that US may be the better choice for examining peripheral nerves (4). The superiority of US was critically analysed and it was added that US is an operator-dependent technology, and the results for US would be probably worse in the hands of a less skilled examiner. Similarly, most MRI studies were performed using a 1.5-Tesla scanner, but many MR-neurographers recommend using a 3-Tesla magnet (8).

1.3. Technical requirements of HRUS

Today, many different scanners are available, including high-quality portable systems, enabling high-end sonographic imaging. Contrast and resolution are the basic physical characteristics of B-mode imaging, and therefore high-resolution linear array transducers are an essential prerequisite for nerve imaging. The scanning frequency used depends on the examined nerve and the clinical question. For superficial nerves, 12-18 MHz is recommended. For imaging of common compression neuropathies, a 12 MHz transducer is usually sufficient, but fine details (such as in post-operative conditions or nerve injuries, e.g. partial dehiscence of a coaptation, small intraneural neuroma) require higher frequencies up to 18 MHz, which gives an axial resolution of 250-500 μm (9). The lateral resolution may reach 0.6 mm. Optimal are multi-frequency transducers with a wide frequency range up to 18 MHz. Image quality depends on spatial and contrast resolution.

Contrast or tissue resolution is defined as the ability to distinguish different normal tissues and normal from abnormal tissues, while spatial resolution refers to the ability to depict and distinguish small objects that are in close proximity. Spatial resolution can be divided into axial and lateral resolution. Axial resolution is defined as the ability to separate two objects lying in tandem along the axis of the ultrasound beam, and lateral resolution as the ability to separate two adjacent objects (10). The use of a 22-MHz high-frequency transducer, which is not usual in the clinical practice, allows the visualization of the inner part of small cutaneous nerves (e.g. the sural nerve) and the measurements of the fascicles, and it could be a valuable tool for evaluating cutaneous nerve neuropathy (11). In dermatology, even higher frequency scanners

operating at frequencies between 20 MHz and 1-2 GHz are available. The optimal frequency range for dermatological questions is between 20 and 100 MHz. Using a 20 MHz transducer, it is possible to visualize structures up to 6-7 mm in depth (12).

Due to the limitation of the penetration depth of high frequencies, for deeper lying nerves (e.g. sciatic nerve) lower frequencies (down to 5 -7.5 MHz) are required. With low ultrasound frequencies, resolution diminishes and the differentiation of nerves from surrounding tissues, as well of their internal structure becomes difficult. Modern ultrasonic scanners allow an assessment of subtle changes up to a depth of about 2.5 cm. Depending on the type of probe and focusing, highest resolution is achieved at a depth of approximately 0.5–1.5 cm from the skin (13). To improve image quality, ultrasound devices are equipped with various software tools. Compound imaging is a tool, which allows the simultaneous recording of several images under different sub-apertures in real time. These single frames are mathematically compounded, resulting in the final image with significant noise reduction and better representation of the tissue boundaries. Furthermore, tissue harmonic imaging (THI) can improve contrast and lateral resolution, and it is therefore especially helpful to visualize deep situated tissue structures. Extended field of view imaging creates a panorama image from numerous individual images, and it can demonstrate complex lesions and document the true extent of the lesion (13). Moreover, high-quality colour-Doppler and duplex function are required to assess nerve vascularisation. This can be useful in nerve tumours, inflammatory nerve diseases, and probably in compressive neuropathies as well. For colour Doppler, a small-flow-setting of the ultrasound device is recommended (pulse repetition frequency 500 Hz, band-pass filter 50 Hz) (7).

The examiner should have a thorough knowledge of the musculoskeletal topographic anatomy, including cross-sectional anatomy. The examiner's expertise in diseases of the peripheral nervous system and electrophysiological knowledge facilitates the correct interpretation of ultrasound nerve pathologies.

1.4. Examination technique with HRUS

Peripheral nerves can be easily identified by means of anatomical landmarks. First, the investigator has to locate anatomical structures such as bones, muscles or

blood vessels lying close to the affected nerve. The examination of peripheral nerves is usually started with transverse sections. Once found, the nerve can be simply traced upwards and downwards in cross-sections. The site of underlying pathology should be examined on longitudinal scans as well.

Nerves and tendons are sonographically characterized by anisotropy. For that reason, the optimal echogenicity of a nerve tissue can only be obtained by a strict perpendicular insonation. In order to further improve the image quality of diagnostic ultrasound, particularly in regions with an uneven body surface (e.g. the elbow), the use of aqueous coupling devices is recommended. As peripheral nerves change their depth during their course in the extremity, the continuous adjustment of the electronic focus as well as of the transmission frequency of the probe is very important. With increasing transmission frequency (and resolution) the penetration depth decreases, and vice versa. Therefore, for example the intrapelvic section of the sciatic nerve cannot be examined with high-resolution sonography. Magnetic resonance tomography here provides superiority. Pathological alterations are always documented in two planes, in longitudinal as well as in transverse scans. Recording short video sequences may provide better understanding of the pathologies. Special questions even require passive movement of the limb to be examined (e.g. snapping triceps syndrome).

In normal-weight people, all major nerves of the extremities, e.g. the median, ulnar, radial, tibial, peroneal, and sciatic nerves can be visualized in their entire course in the extremities. Even smaller nerves of the upper extremity, e.g. the posterior interosseus, superficial radial, musculocutaneous and cutaneous antebrachii nerves, the palmar branch of the median nerve, the superficial and deep branch of the ulnar nerve at the wrist level can be readily displayed. The imaging of the axillary nerve is troublesome because of its rather complex course through several soft tissue compartments of the shoulder and axilla. However, using reliable anatomical landmarks it could be detected in all 15 examined persons (14). Even nerves of the trunk and abdominal wall, e.g. thoracodorsal nerve, long thoracic nerve, intercostal nerves, ilioinguinal nerve, iliohypogastric and genitofemoral nerves, obturator nerve and pudendal nerve can be examined (9). The spinal nerves C4-C8 and the supraclavicular brachial plexus can also be visualized, but especially the inferior trunk and the fascicles are not constantly imaged in good quality. The visualization of the infraclavicular and

infrapectoral brachial plexus is restricted by the clavicle and the depth of the structures. Cranial nerves, such as the vagal and accessory nerves, can be easily visualized at the level of the neck. Particularly in obese patients, the examination of the sciatic nerve in the thigh and the tibial nerve on the proximal lower leg is difficult or even impossible. In thin individuals, however, even small sensory nerves on the lower extremity, such as the saphenous nerve, sural nerve, superficial peroneal nerve, lateral femoral cutaneous nerve and lateral cutaneus suralis nerve can be assessed (9).

1.5. Ultrasound anatomy of the normal peripheral nerve

The cross sectional appearance of the normal peripheral nerve is round to oval and reminiscent of a honey comb (*Fig .2*).

Figure 2. Honey comb appearance of the median nerve at the distal forearm on transverse scan 1 cm under the surface. Cross-sectional area is (CSA) 0.08 cm² (Toshiba Aplio T-500, 18 MHz linear array).

The hypoechogenic fascicles are surrounded by an echogenic rim representing the interfascicular epineurium and the perineurial sheath. Fascicles are the smallest

structure to be visualized by HRUS, individual axons and the endoneurium are not visible. The outer hyperechogenic layer is the outer epineurium. Particularly in large nerves, a clear cable-like fascicular echotexture can be seen.

The number of fascicles depends on the type of the nerve (amount of motor and sensory fibres), its location and its size. The amount of the fascicles varies in the course of the nerve, because they repeatedly unite and divide. Depending on the transmission frequency and resolution of the probe, the number of fascicles in the ultrasound image can differ from that determined histologically (15). This may be explained by the coalescence of some adjacent fascicles in a single image (13). In longitudinal sections, peripheral nerves have a cable-like appearance, in contrast to the more fibrillar echotexture of tendons. In addition, tendons can be easily distinguished from nerves sonographically, because they end in a muscle proximally.

Peripheral nerves at the root level have a mono-fascicular architecture, subdividing into a fascicular group arrangement more distally, eventually reaching a multi-fascicular arrangement in the periphery. Parallel with this changing group arrangement, the amount of connective tissue between the fascicles (inter fascicular epi- and perineurium) increases. This explains the fact why cervical roots demonstrate only one individual fascicle in sonography, whereas the number of fascicles for example in the median nerve increases from proximal to distal.

With the colour Doppler and duplex function of current ultrasound equipments, epineural vessels can also be identified. As quantitative diagnostic criteria for “hypervascularization” are not yet available, the affected side should be compared with the unaffected one.

Many disorders of peripheral nerves result in an increase of nerve size. These conditions include entrapment, other mononeuropathies of various aetiologies, polyneuropathies, trauma, and nerve tumours. Ultrasonography allows precise structural analysis and quantitative measurements of the nerves, which makes comparison of different studies possible. Nerve width (medial to lateral diameter), thickness (anterior to posterior diameter) and cross-sectional area (CSA) measured on transverse scans, and antero-posterior diameter (LAPD) measured on longitudinal scans are the most frequently used quantitative parameters for the ultrasound investigation of peripheral nerves. Furthermore, ratios of CSA between different segments of the same nerve have

also been used (16, 17). CSA reference values for some peripheral nerves and the brachial plexus have been reported in previous studies (18-22, 33).

2. OBJECTIVES

Nerve size change is one of the most important ultrasonographic features of nerve pathology. Therefore it is crucial to have normal (reference) values of all nerves routinely assessed. Furthermore, in order to be able to use these reference values with confidence in everyday practice, it is also important to examine the reliability of these normal values, i.e. the congruence of values obtained by different examiners, ultrasound devices and by the same examiner at different time points.

Several reports have been published on reference values for the cross-sectional area of the median nerve. This resulted in an evidence-based guideline stating that ultrasound may be used as a diagnostic test for carpal tunnel syndrome (Level A). There are also several reports on reference values for the CSA of the ulnar nerve with good agreement among the measurements, among them some recent studies (24, 25). On the other hand, data are less abundant concerning normal values for cervical roots, radial nerve, lower limb nerves and pure sensory nerves, as mentioned above, and they show more variation. The **first objective** of our study was to establish a set of normal CSA values for C5, C6, and C7 cervical roots, and several upper and lower limb nerves, including some pure sensory nerves, at pre-defined anatomical sites, and to assess whether CSAs correlated with age, gender, height, and body weight. Our **second objective** was to systematically assess the reliability of these measurements on several nerves in the upper and lower limbs, with respect to intra-rater, inter-rater and inter-equipment variation. CSA values of two independent cohorts from the two study sites were also compared in order to determine the external validity of collected normal values.

A large body of ultrasonographic literature is available on common neuropathies such as carpal tunnel syndrome and ulnar neuropathy at the elbow, but literature data on uncommon conditions are lacking. As the **third objective** of our study, we analysed

cases of rare neuropathies assessed by ultrasonography in order to establish the role of HRUS in rare disorders of the peripheral nerves.

3. METHODS AND PATIENTS

3.1. Normal values and reliability assessments

Subjects

Prior to the start of our study, approval of the institutional review board at both study sites was obtained, and participants signed informed consent. Between May 2011 and December 2011, 56 healthy subjects were investigated with high-resolution nerve ultrasound at the Dept. of Neurology of Semmelweis University in Budapest (Hungary) and at the Dept. of Neurology of the District Hospital in Freiberg (Germany). Subjects were recruited from the hospital staff and patients. None of the study subjects had symptoms or signs suggesting polyneuropathy or systemic diseases potentially associated with polyneuropathy, nor any history of neuromuscular disease. Demographic data (age, gender, height, and body weight) were recorded. All subjects were of Caucasian ethnicity. For the inter-rater reliability assessments in addition to the healthy subjects patients from a polyneuropathy study in Budapest have been included.

Ultrasound examination

For ultrasound examinations, a Philips HD15XE ultrasound device with a small part imaging software and a 15 MHz 3 cm “hockey stick” linear array transducer was used for 25 subjects in Budapest. In Freiberg, the same device was used for 10 subjects, and an additional 21 subjects were examined with a Toshiba Aplio SSA-700A device with small part imaging software and a 12 MHz PLT-1204 4.5 cm linear array transducer. In both devices, compound imaging software (*SonoCT* for the Philips HD15XE and *ApliPure* for Toshiba Aplio SSA-700A) was used to improve image quality.

Normal value measurements

The following 14 CSA measurements (*Fig. 3*) on the upper and lower extremities were carried out, all on the left side: C5, C6 and C7 cervical roots; median, ulnar and radial nerves at the mid-upper arm; ulnar nerve at the elbow at the level of the medial epicondyle, median, ulnar and superficial radial nerves at the distal third of the forearm; median nerve at the proximal entrance of the carpal tunnel; peroneal nerve at the fibular neck; tibial nerve at the ankle; and sural nerve at the proximal calf. The measurements were time-consuming (approximately 45-55 minutes) and therefore they have been performed only on the left side. These sites included common areas of nerve entrapment (ulnar nerve in the ulnar groove, median nerve in the carpal tunnel), sites largely inaccessible for electrophysiologic studies (cervical roots), as well as sites corresponding to those usually evaluated by electrodiagnostic studies. The superficial radial and the sural nerves were chosen as pure sensory nerves. Subjects were examined mostly in supine position, with the exception of the peroneal nerve examined with the subject lying on one side, and the sural nerve examined in prone position.

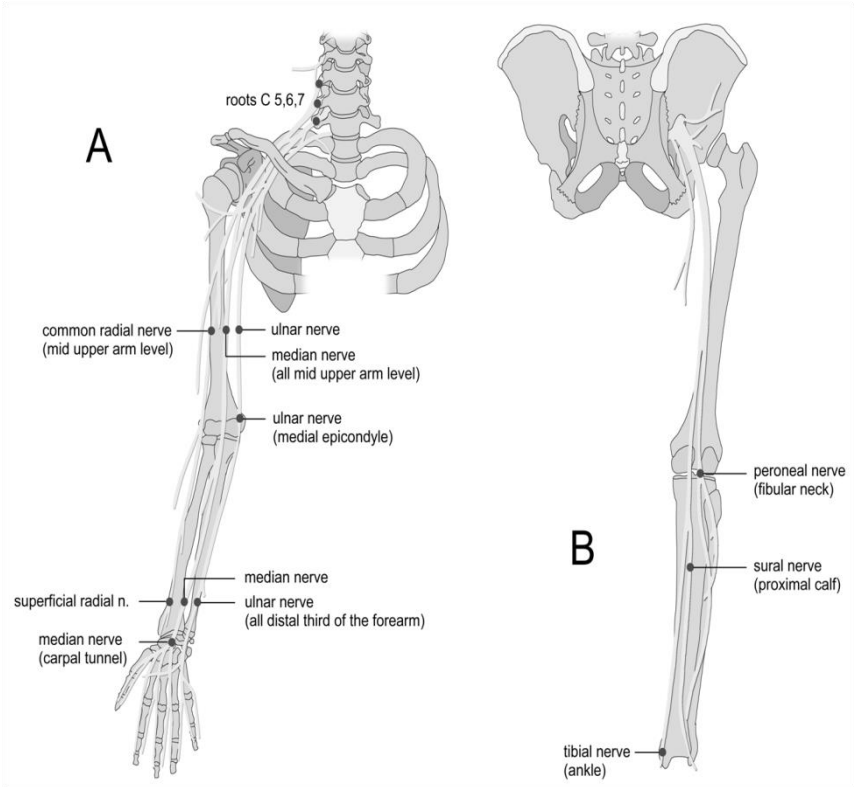

Figure 3. Anatomical landmarks used for peripheral nerve ultrasound measurements in the study.

For brachial plexus sonography, the following technique described earlier for determining root level was used (26): The C7 root was identified in the oblique transverse plane of the C7 vertebra, which appeared as a hyperechoic structure characterized by the presence of only a posterior tubercle on its transverse process, the anterior tubercle being absent. When the transducer was moved slightly upward, the C6 and C5 vertebrae were successively identified by the presence of both anterior and posterior tubercles, the C5, C6 roots appearing as hypoechoic structures between the tubercles. Colour Doppler sonography was used to differentiate roots from blood vessels.

The nerves of the upper and lower extremities were identified on transverse scans using the same typical anatomic landmarks as described before (27). On the upper arm, the median nerve was identified adjacent to the brachial artery between the biceps and triceps muscles at the midpoint of the line connecting the axilla and the medial epicondyle. The ulnar nerve was then identified at the same level by moving the probe more medially. The radial nerve was assessed at the same level directly on the surface of the humerus in the radial nerve groove, accompanied by the deep brachial artery. At the elbow, the ulnar nerve was measured in the ulnar groove, with the elbow in a slightly flexed position, between the medial epicondyle and the olecranon. On the distal forearm, the median nerve was measured first at the level of the proximal third of the pronator quadratus muscle: after the pronator quadratus muscle was visualized, the median nerve was identified between the tendons of the flexor pollicis longus and flexor digitorum superficialis muscles. From this point, the transducer was moved medially to the ulnar nerve, which is accompanied at this level by the ulnar artery. Next, the transducer was moved radially to identify the superficial radial nerve, lying between the extensor carpi radialis longus and flexor carpi radialis muscles, just above the palpable bony prominence of the radius, and adjacent to the radial artery (28). At the wrist, the median nerve was examined at the proximal entrance of the carpal tunnel using the pisiform bone as an anatomic landmark.

On the lower limb, transverse scan of the peroneal nerve was obtained at the level of the fibular neck with the subject lying on the side, and the knee propped up and slightly flexed (20° to 30°) (27). The tibial nerve was examined at the level of the

medial malleolus, just posterior to the tibial artery. The sural nerve was examined at the proximal dorsal calf, identified superficially between the two heads of the gastrocnemius muscle. If necessary for correct identification, the nerve was followed more distally.

The CSA of the nerves was measured using the trace function of the ultrasound device by manually tracing inside the hyperechoic rim of each nerve (*Fig. 4*). The angle of insonation was adjusted perpendicular to the nerve where the nerve appeared the brightest with the best discernible outer margins. The CSA of each nerve segment was measured three times. The three measurements were averaged and the mean value was used for analysis.

Reliability assessments

The *inter-rater reliability* was assessed at the start of the study. Two ultrasonographers measured nerve cross-sectional areas in 7 subjects (on all 14 sites in each subject, as described above). Both examiners are neurologists and clinical neurophysiologists who perform neuromuscular ultrasound in a clinical setting on a daily basis. Both ultrasonographers received training for this study prior to the initiation of data collection. The repeated measurements were done in one session: the examination of all 14 nerve segments by one rater was repeated in the same session by the other rater who was blinded to the results of the first.

To assess *intra-rater reliability*, 6 subjects in Freiberg were re-examined with the same Toshiba device by the same investigator 24 hours after the first sonographic examination.

To assess *inter-equipment reliability*, 6 subjects in Freiberg were examined by the same examiner first with the Philips, and 8-11 weeks later with the Toshiba ultrasound device.

The *validity of normal values* was tested by comparing CSA values of the 14 nerve segments in the two independent cohorts of the two study sites.

Statistical analysis

Descriptive statistics were used to present basic demographic data of the study population. The following parameters were calculated and presented for normal CSA values of the 14 nerve segments: mean, median, standard deviation (SD), 95%

confidence intervals of the mean, and the coefficient of variation. Normality of variables was checked by the Shapiro-Wilk test. Correlation of CSA measurements with age, gender, height and body weight was tested using the Spearman correlation coefficients. Values between genders were compared by the Kruskal-Wallis ANOVA. The general linear model (GLM) was used to test if gender remains a significant predictor of CSA when age, height and body weight are also considered. Intraclass correlation coefficients and corresponding 95% confidence intervals were calculated to define values for intra-rater, inter-rater, and inter-equipment reliability. The validity of our normal values was tested in two independent cohorts using repeated measure ANOVA for the comparison of CSA values of the 14 nerve segments. Statistica for Windows v. 11 (StatSoft, Tulsa, OK) was used for data analysis.

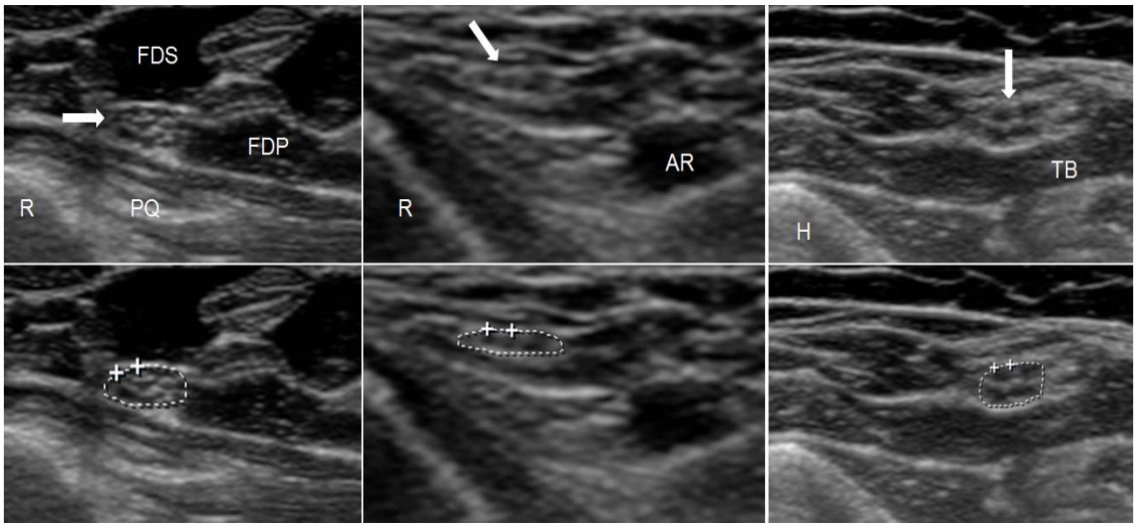

Figure 4. Normal ultrasound images of three different nerves. On the lower images, the tracing used to measure the cross sectional area is shown.
Left: Median nerve at the distal forearm (CSA: 7.7 mm²); R= radial bone, PQ= pronator quadratus muscle, FDS= flexor digitorum superficialis muscle, FDP= flexor digitorum profundus muscle. Arrow points to the median nerve.
Middle: Superficial radial nerve at the distal forearm (CSA: 1.9 mm²); R= radial bone, AR= radial artery. Arrow points to the superficial radial nerve.
Right: Ulnar nerve at the upper arm (CSA: 6.8 mm²); H=humerus, TB= medial head of the triceps brachii muscle. Arrow points to the ulnar nerve.

3.2. Ultrasonography of patients with rare neuropathies

Subjects

Between January 2009 and December 2013, about 3500 predominantly outpatients were investigated with HRUS at the Dept. of Neurology of the District Hospital in Freiberg (Germany). The vast majority of the patients were adults. The patients were referred to the outpatient consultation with a suspected peripheral nerve disease from different faculties, mostly surgeons (trauma surgeons, neurosurgeons, hand surgeons), neurologists and general practitioners. All patients were examined neurologically and by standard electrodiagnostic examination, consisting of nerve conduction studies, recording of late responses (F-waves) and needle electromyography. Demographic data (age, gender, height, and body weight) were recorded.

Ultrasound examination

For ultrasound examinations between January 2009 and November 2012, a Toshiba Aplio SSA-700A device with small part imaging software and a 12 MHz PLT-1204 4.5 cm linear array transducer and from November 2012 a Toshiba Aplio T-500 SSA-700A device with small part imaging software and a 18 MHz array transducer was used. In both devices, compound imaging software (*ApliPure)* was used to improve image quality.

Ultrasound measurements

Depending on the clinical question, either a single nerve was examined, mostly bilaterally in order to ascertain side differences, or in suspected generalized diseases several nerves were examined on different segments along the course of the nerve. Pathological alterations were documented in two planes, in longitudinal as well as in transverse scans. Occasionally, short video sequences were recorded for better understanding of the pathology.

The CSA of the nerves was measured using the trace function of the ultrasound device by manually tracing inside the hyperechoic rim of each nerve.

4. RESULTS

4.1. Normal values and reliability assessments

Basic demographic features of the study population are given in *Table 1*.

Table 1. Demographic data of the two study cohorts

Parameter	Germans	Hungarians	P
N	31	25	-
Age (years)	51.8±16.4	48.5±15.6	0.45
Gender (M:F)	15:16	11:14	0.74
Weight (kg)	75.4±13.0	79.6±18.2	0.31
Height (cm)	171±9	168±6	0.12

No difference in demographic features between the Hungarian and the German study groups

The univariate relationships between CSA and age, body weight, height and gender are presented in *Table 2.* The results of multivariate testing for the effect of gender are presented in the last column of *Table 2*. CSA measurements showed mostly normal distribution in both genders and in pooled data.

Descriptive statistics of CSA measurements of all 14 nerve segments for all subjects are presented in *Table 3*. Mean CSA values of these 14 nerve segments ranged from 2 to 10 mm^2 (*Table 3* and *Fig. 8*).

Table 2. Univariate Spearman correlations of peripheral nerve CSA values with age, body weight, height, and Kruskal-Wallis ANOVA test for gender, and multivariate testing (GLM) for gender

Nerve/Site	Age		Weight		Height		Gender	
	Spearman R	p	Spearman R	p	Spearman R	p	p for K-W	p for GLM*
C7	0.01	0.95	0.11	0.45	0.08	0.57	0.76	0.89
C6	0.37	***0.006***	-0.10	0.46	0.04	0.76	0.19	0.31
C5	0.16	0.27	-0.05	0.74	-0.12	0.41	0.18	0.91
Median arm	0.28	***0.035***	0.05	0.74	0.15	0.25	***0.02***	0.08
Ulnar arm	0.21	0.12	0.12	0.38	0.07	0.62	***0.03***	***0.03***
Radial arm	0.04	0.79	0.29	***0.03***	-0.01	0.96	***0.04***	***0.001***
Ulnar epicond	0.26	0.051	0.18	0.19	0.03	0.84	0.24	0.27
Median forearm	0.04	0.75	0.04	0.78	-0.10	0.45	0.41	0.11
Ulnar forearm	0.36	***0.007***	0.20	0.15	-0.03	0.84	0.61	0.78
Spf radial forearm	0.46	***0.001***	0.21	0.11	-0.01	0.99	0.06	0.21
Median carpal	0.06	0.66	0.18	0.18	0.08	0.58	0.17	0.06
Peroneal	-0.03	0.83	0.41	***0.001***	0.18	0.18	0.25	0.50
Tibial	0.19	0.16	0.35	***0.008***	0.31	***0.02***	***0.02***	0.23
Sural	-0.02	0.87	0.03	0.83	-0.31	***0.03***	0.27	0.53

CSA=cross-sectional area; Spf=superficial Values are uncorrected for multiple comparisons. K-W: Kruskal –Wallis univariate ANOVA for comparing CSA values between genders.

*GLM: general linear model analysis, taking gender, age, weight and height as possible predictors of CSA. P values for gender are presented with correction for age, height and weight.

Table 3. CSA values (mm^2) of 14 nerve segments in 56 healthy subjects

Nerve/Site	Valid N	Mean (mm^2)	Median (mm^2)	SD (mm^2)	95% CI for the mean (mm^2)	Coeff. of var. (%)
C7	50	**10.0**	**10.0**	2.9	9.1 – 10.8	29.5
C6	50	**9.5**	**8.7**	2.7	8.7 – 10.2	28.1
C5	52	**5.6**	**5.3**	1.6	5.1 - 6.0	29.1
Median arm	56	**8.9**	**8.9**	1.8	8.4 – 9.4	20.7
Ulnar arm	56	**6.3**	**6.3**	1.7	5.8 – 6.8	27.1
Radial arm	56	**4.2**	**4.1**	1.0	3.9 - 4.5	24.2
Ulnar epicond	56	**7.6**	**7.3**	2.1	7.0 - 8.1	27.3
Median forearm	56	**5.7**	**5.9**	1.3	5.4 - 6.0	22.2
Ulnar forearm	56	**5.2**	**5.0**	1.3	4.9 - 5.6	25.7
Spf radial forearm	56	**2.3**	**2.0**	0.7	2.1 - 2.5	31.2
Median carpal	56	**8.5**	**8.4**	1.8	8.0 - 9.0	21.4
Peroneal	56	**8.9**	**8.8**	2.0	8.3 - 9.4	23.1
Tibial	56	**9.6**	**9.1**	2.2	9.0 - 10.2	23.4
Sural	50	**1.8**	**2.0**	0.6	1.6 - 1.9	35.7

CSA=cross-sectional area; Spf=superficial; SD=standard deviation; CI=confidence interval; Coeff. of var.=Coefficient of variation

Inter-rater reliability, *intra-rater* test-retest reliability, and *inter-equipment* test-retest reliability are presented in *Figs. 5-7.* Intraclass correlation coefficients in all three analyses of reproducibility were remarkably high (0.86 – 0.98).

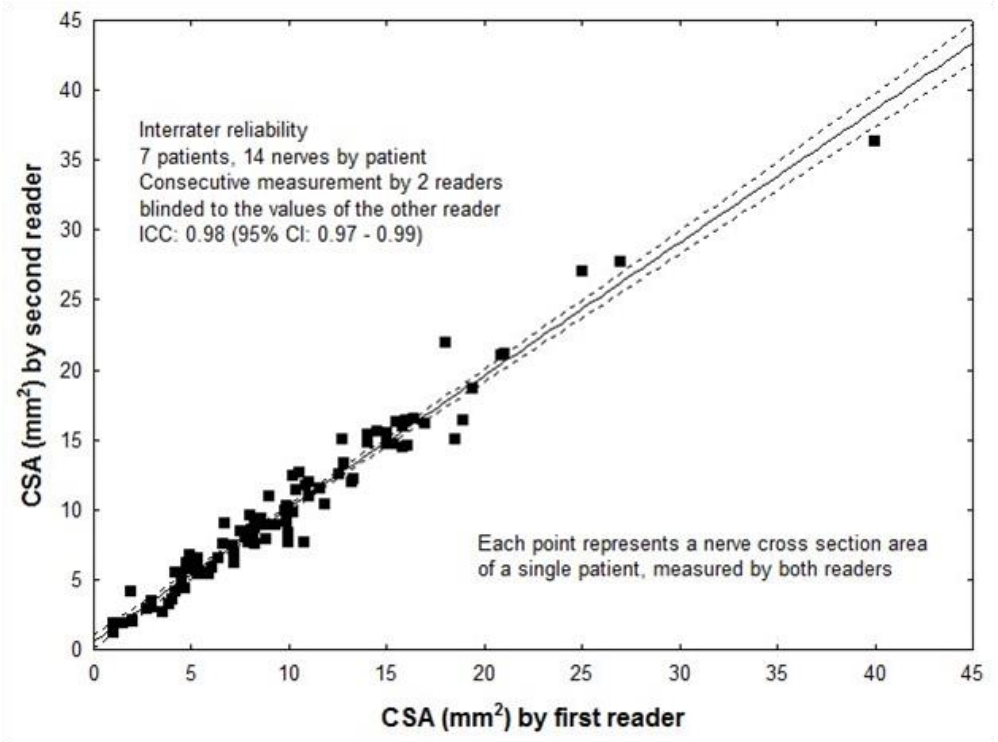

Figure 5. Inter-rater reliability**.** CSA measurements of 14 segments by two raters within one session. The second rater was blinded to the measurements of the first.

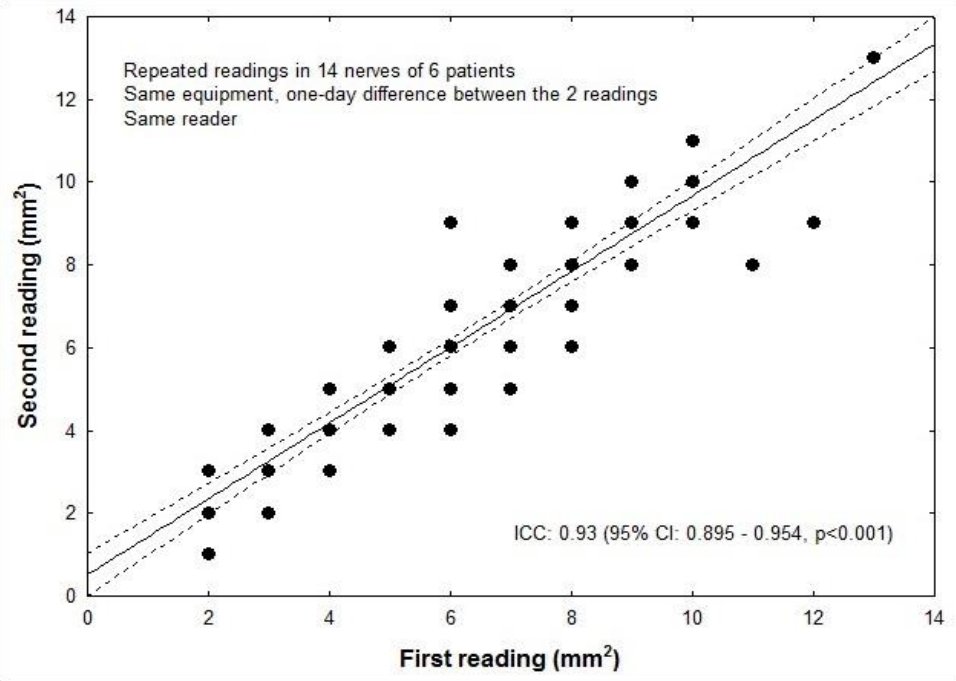

Figure 6. Intra-rater test-retest reliability**.** Repeated measurements by the same reader of 84 nerves in 6 patients one day apart. Due to the overlap, only 34 out of 84 datapoints appear in the plot.

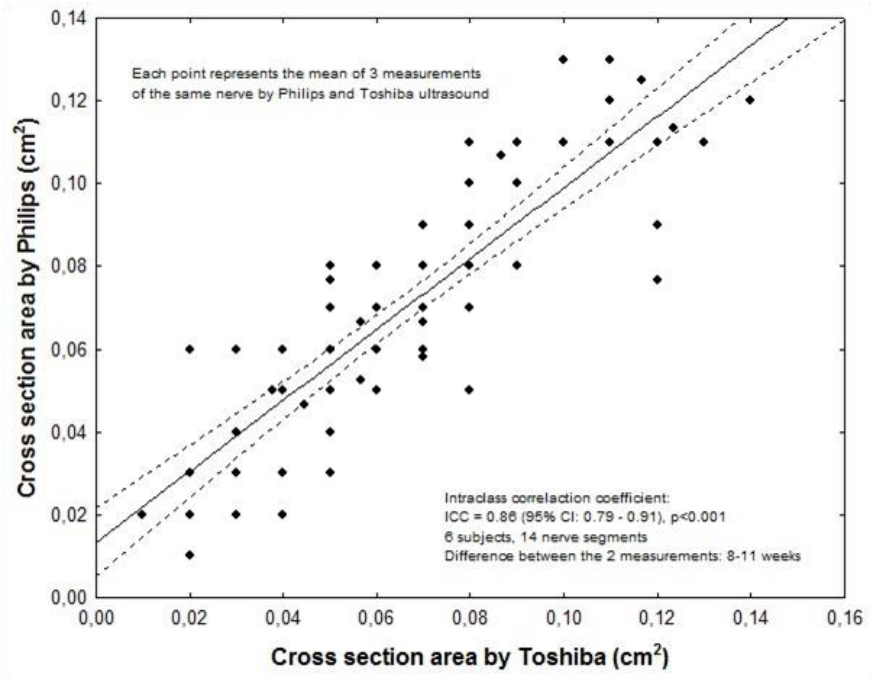

Figure 7. Inter-equipment test-retest reliability**.** Repeated readings by the same reader of 84 nerves in 6 patients with two different equipments, within 8-11 weeks. Some of the datapoints overlap.

When CSA values of the 14 nerve segments were compared between two independent cohorts, no significant difference was found (*Fig. 8*).

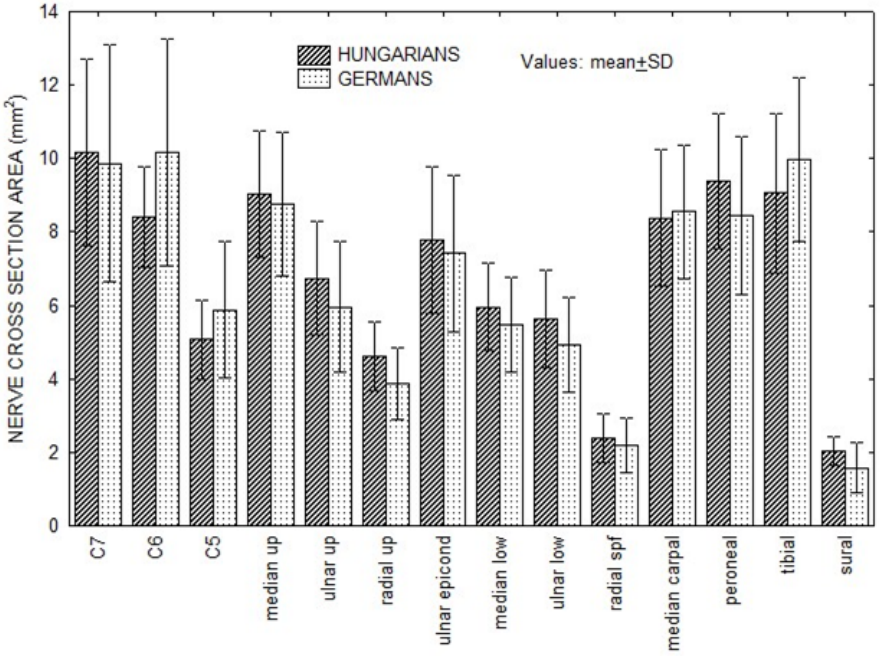

Figure 8. Measurements in two independent cohorts. CSA values of 14 nerve segments in Hungarian (N= 25) and German (N=31 healthy subjects). Repeated measure ANOVA revealed no significant country effect. When pairwise comparisons were done by the Mann-Whitney-test, no significant difference was found between the CSAs in any of the nerve segments after correction for multiple comparisons.

4.2. Ultrasonography of patients with rare neuropathies

4.2.1. RARE TUMOURS AND FOCAL TUMOUR-LIKE LESIONS

Case 1. Amyloidosis

In a 68-year-old female patient with progressive radial nerve lesion with paresis distal to the triceps muscle, electrodiagnostic testing revealed axonal motor and sensory lesion, but the exact level of the lesion could not be ascertained. 1.5 T-MRI findings were negative. By means of high resolution ultrasound, a hypoechoic lesion of the

common radial nerve was identified, involving its complete course from the axilla to the spiral groove, with marked segmental enlargement (CSA=0.62 cm², diameter 7.6 mm) at the distal part of the spiral groove. In this segment, sonography indicated the presence of calcification which was later histologically confirmed to be a small metaplastic ossification. Furthermore, fascicular biopsy revealed amyloid deposition using congo red stain and polarized light microscopy *(Fig. 9*). Because neither laboratory findings nor histology (nerve and rectum) could reveal a primary light chain amyloidosis (AL), we could not confirm a primary amyloidosis in this case. Curative surgical treatment by means of microsurgery was impossible.

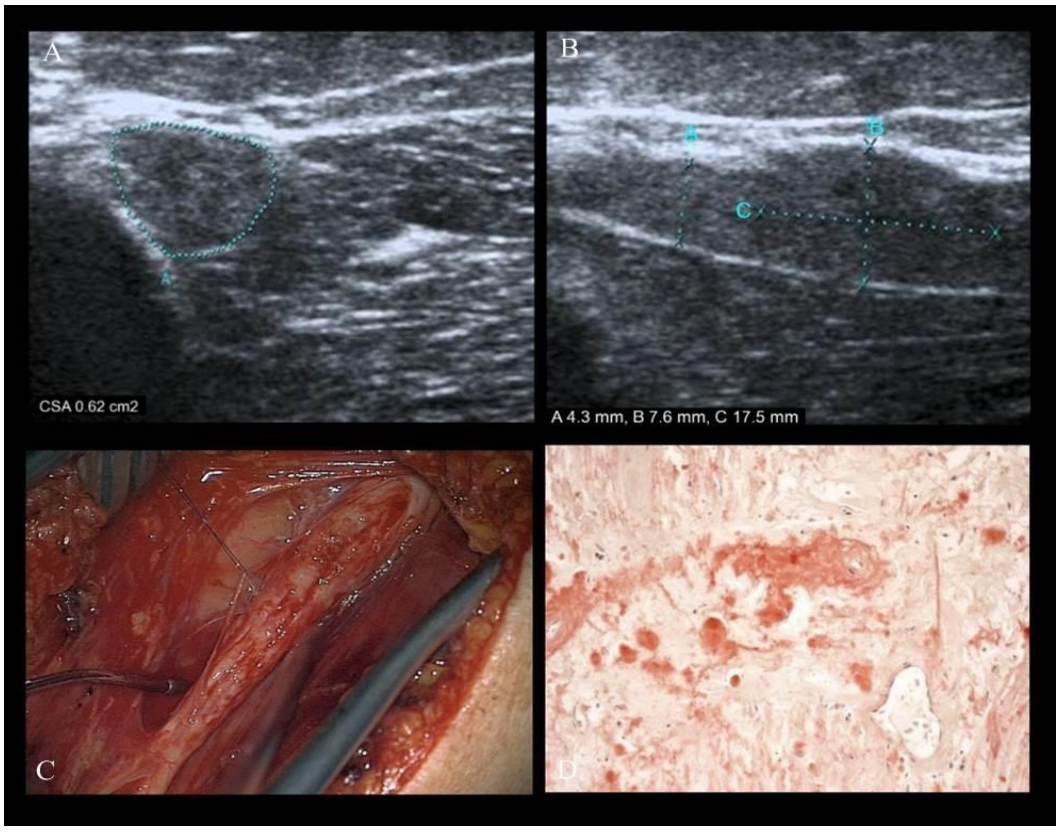

Figure 9. Affection of the common radial nerve by amyloidoma. HRUS on transverse scan (A) and longitudinal scan (B) demonstrates a focal, hypo-echoic nerve enlargement with effacement of the fascicles. Intraoperative image (C) shows a fusiform nerve enlargement. Fascicular biopsy was carried out. Courtesy of TN Lehmann, MD (Department of Neurosurgery, Bad Saarow/Germany) Histological examination (D) revealed amyloid deposition. Courtesy of S Koch, MD PhD (Department of Pathology, Bad Saarow/Germany).

Case 2. Intraneural lymphoma

In a 70-year-old female patient after 2 years of progressive ulnar neuropathy, unsuccessful neurolysis of the nerve at the elbow was performed. MRI (1.5 T) at the elbow showed an enlarged ulnar nerve. HRUS demonstrated a large inhomogeneous, mostly hypoechogenic nerve lesion. Its contour on longitudinal scan was slightly irregular with some hypervascularisation of the nerve from the axilla to the elbow (*Fig. 10*). Another vascularized tumour was seen within the flexor carpi ulnaris muscle. Histology revealed primary non-Hodgkin's B-cell lymphoma with additional axillary and supraclavicular lymph node metastases.

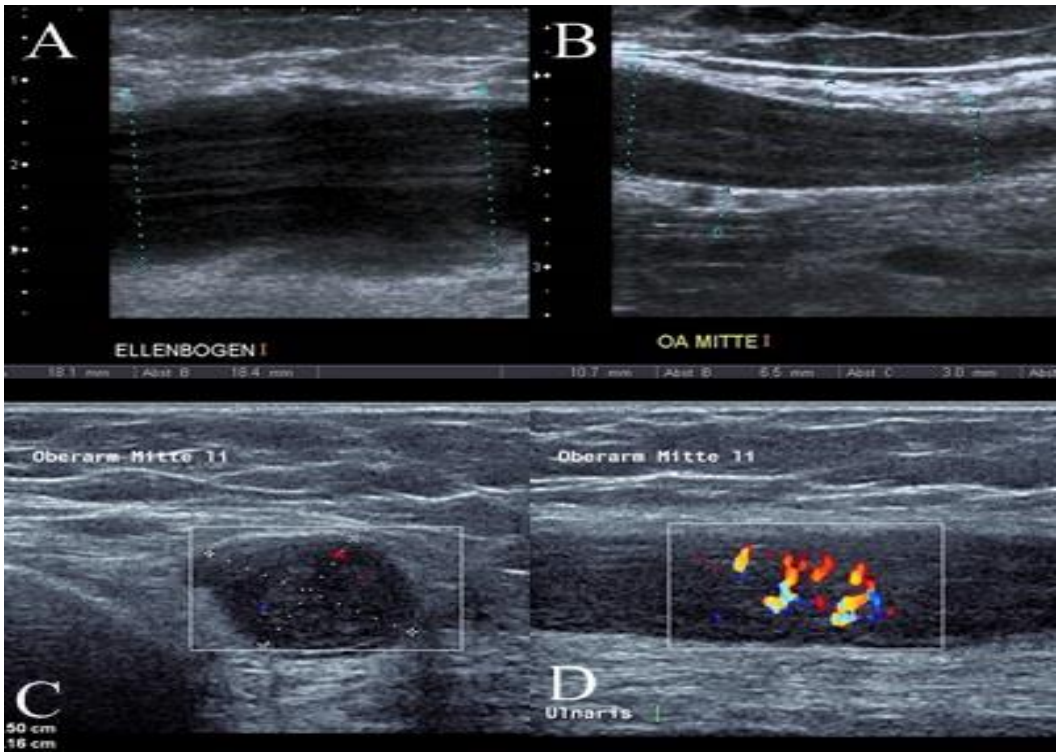

Figure 10. Affection of the ulnar nerve by intraneural lymphoma. HRUS (A) demonstrates a large hypoechoic nerve enlargement without fascicular structure on longitudinal view at the elbow (A) and at the middle-arm (b). At the mid-arm level on transverse scan (C) and on longitudinal scan (D) intraneural hypervascularisation.

Case 3. Radial nerve lesion in rheumatoid arthritis

In a 32-year-old female patient during the first trimester of pregnancy, after discontinuation of the treatment with sulfalazin and dose reduction of prednisolone from 7.5 mg to 5 mg/day given for rheumatoid arthritis, painless radial nerve palsy without

involvement of the triceps muscle developed. No signs of inflammation were present. Electrodiagnostic testing showed axonal radial nerve lesion of distal upper arm type. EMG demonstrated denervation signs not only in the muscles innervated by the posterior interosseus nerve but also in the brachioradial and the extensor carpi radialis muscles, which indicated that the lesion started somewhat distal to the triceps muscle.

HRUS demonstrated (*Fig. 11*) short focal enlargement of the radial nerve on the upper arm distal to the spiral groove with prominent fascicles (CSA: 0.11 cm²; diameter: 2.7 mm; diameter on the contralateral side: 1.5 mm). Spontaneous recovery ensued over 6 months without increasing the dose of the drugs again.

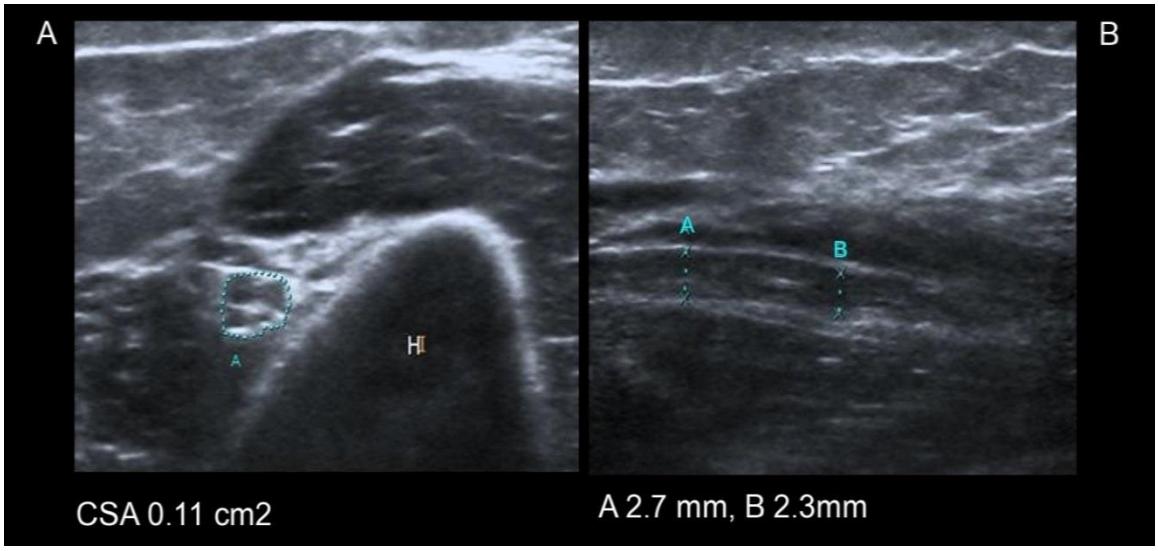

Figure 11. Radial nerve distal to the spiral groove between the brachioradial and the brachial muscles (H= Humerus) with a CSA of 0.11 cm² on transverse scan (A) with prominent fascicular structure and longitudinally enlarged nerve (2.7 mm) (B).

Case 4. Plexiform neurofibromatosis

In a 27-year-old male patient, progressive painless radial nerve palsy developed over the course of one year. Steroids and immunoglobulins were ineffective. Clinical examination and electrodiagnostic testing indicated a lesion distal to the triceps muscle. 1.5 T-MRI was negative. HRUS demonstrated (*Fig. 12*) a lesion of the radial nerve without vascularization - more proximally than suggested clinically and electrophysiology - between the axilla and the spiral groove (CSA: 0.42 cm²; extensive

hypoechogenic elongation: 4 mm). Histology after operation demonstrated a plexiform neurofibroma.

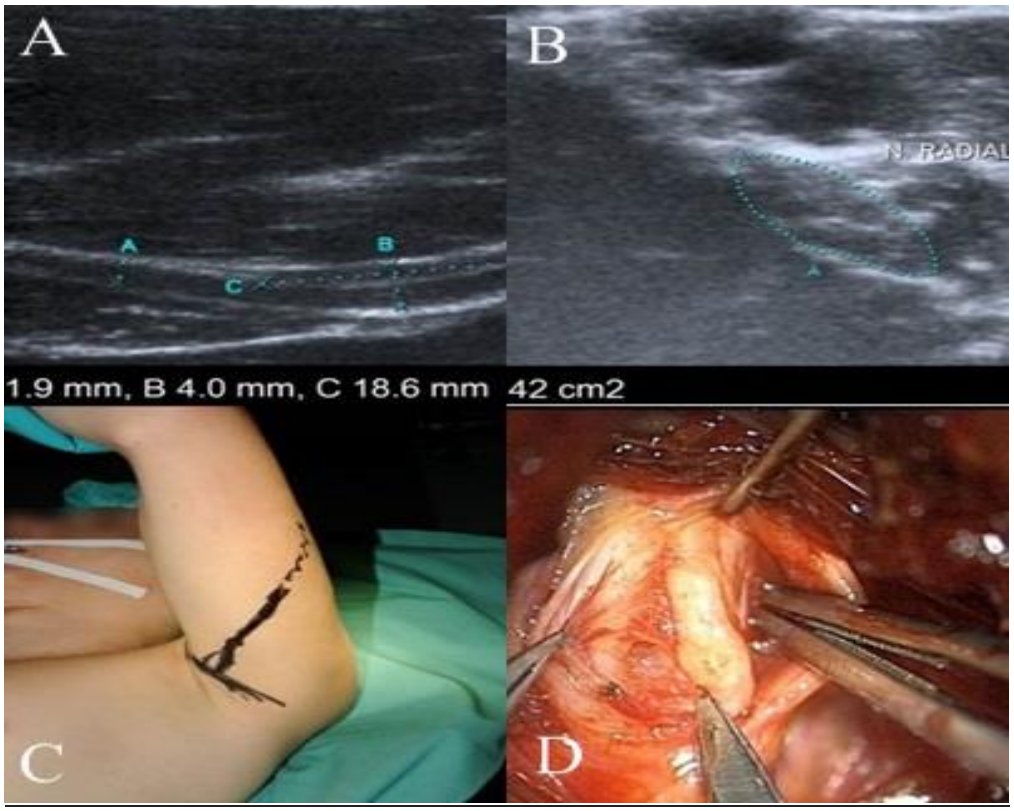

Figure 12. Extensive enlargement (4 mm) of the radial nerve proximal to the spiral groove without evidence of vascularization on duplex (A).CSA (0.42 cm²) was increased (B). Operation site (C), markedly enlarged nerve nerve after epineurotomy (D). Image (C, D) courtesy of TN Lehmann, MD (Department of Neurosurgery, Bad Saarow/Germany).

4.2.2. NERVE TORSION

A 42-year-old male patient had a 15-month-long history of numbness on the ventral upper arm with severe pain for 2 weeks in the mid-upper arm, radiating one week later to the thumb. Possibly mechanical stress (intensive training with dumbbells) was reported. Neurological examination showed sensorimotor deficit of the radial nerve of distal upper arm type (triceps muscle intact, brachioradial muscle without voluntary activation). Electrodiagnostic testing after 3.6 and 12 months showed no signs of

reinnervation on EMG. 1.5 T-MRI was negative. HRUS demonstrated an enlarged nerve (CSA= 0.20 cm²), a caliber change with an hourglass-like constriction and a change in the continuity of the epineurium indicating a possible torsion of the nerve with a long segment increase of the diameter, proximally (3.6 mm) more than distally (*Fig. 13A*). On the contralateral side, the diameter of the radial nerve was normal (1.7 mm). The deep brachial artery just above the constriction showed normal flow characteristics.

Intraoperatively, the radial nerve was found to be twisted and constricted after the removal of the adventitia (*Fig.13B*). A pseudoneuromatous bulging mostly proximal to it was discernable. The surgical approach consisted of microsurgical exploration by means of epineurotomy as a first step. A careful derotation followed, a procedure, which was already reported rather early as helpful (29), but this case needed subsequent segmental resection and repair by grafts in accordance with literature cases (30).

Histology showed pronounced neural fibrosis at the level of the torsion and some inflammatory cell infiltration of the neighbouring nerve fascicles.

The operation was carried out 15 months after onset of the symptoms. Slight electrophysiological and clinical recovery of the radial nerve was noticed 4 months after surgery**.** HRUS showed a new torsion distal **(***Fig. 13C)* to the site of the first torsion, which was again confirmed by neurosurgical exploration**.**

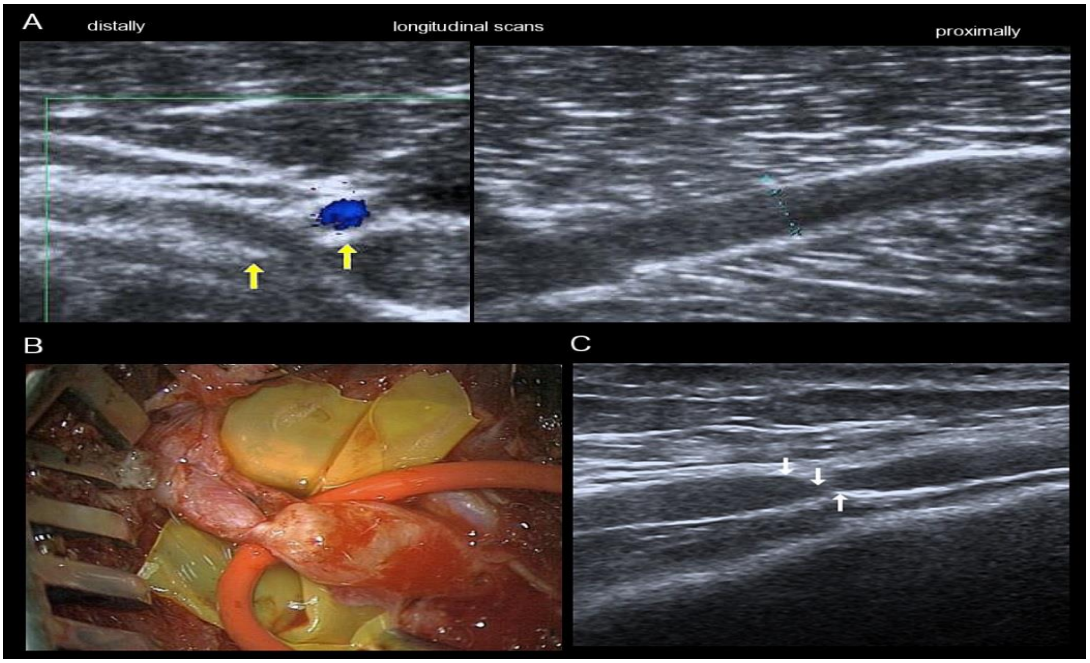

Figure 13. HRUS with multiple torsions of the radial nerve. A: Substantial calibre change and hourglass-like constriction (arrows) with deep brachial artery just above the constriction as well as long-segmental enlargement of nerve diameter proximal to the constriction (3.6 mm). B: Corresponding intraoperative image. The twisted constriction and proximal bulging of the nerve was clearly seen only after removal of adventitia. Image courtesy of TN Lehmann, MD (Department of Neurosurgery, Bad Saarow/Germany). C: A second distally located spontaneous torsion of the radial nerve in the same patient 12 months after surgical repair of the torsion depicted in A and B.

4.2.3. RARE DISEASES MIMICKING CARPAL TUNNEL SYNDROME

Case 1. Thrombosis of the persistent median artery mimicking carpal tunnel syndrome

A 40-year-old right-handed locksmith complained of pain in the whole hand during the day mainly after manual work with pain relief during the night for the last three months. He reported mild dysesthesia on the median nerve innervated fingertips. Phalen-test was negative. The pulse of radial and ulnar artery was normal. Electrodiagnostic testing showed normal values. HRUS showed a normal median nerve in the carpal tunnel with normal echotexture and CSA on transverse scan. No compression signs (no caliber change on the longitudinal scan) (*Fig. 14A*), but an enlarged, partly coloured persistent median artery was seen on duplex-sonography (*Fig. 14B*). The vessel was not compressible and showed no pulsation .

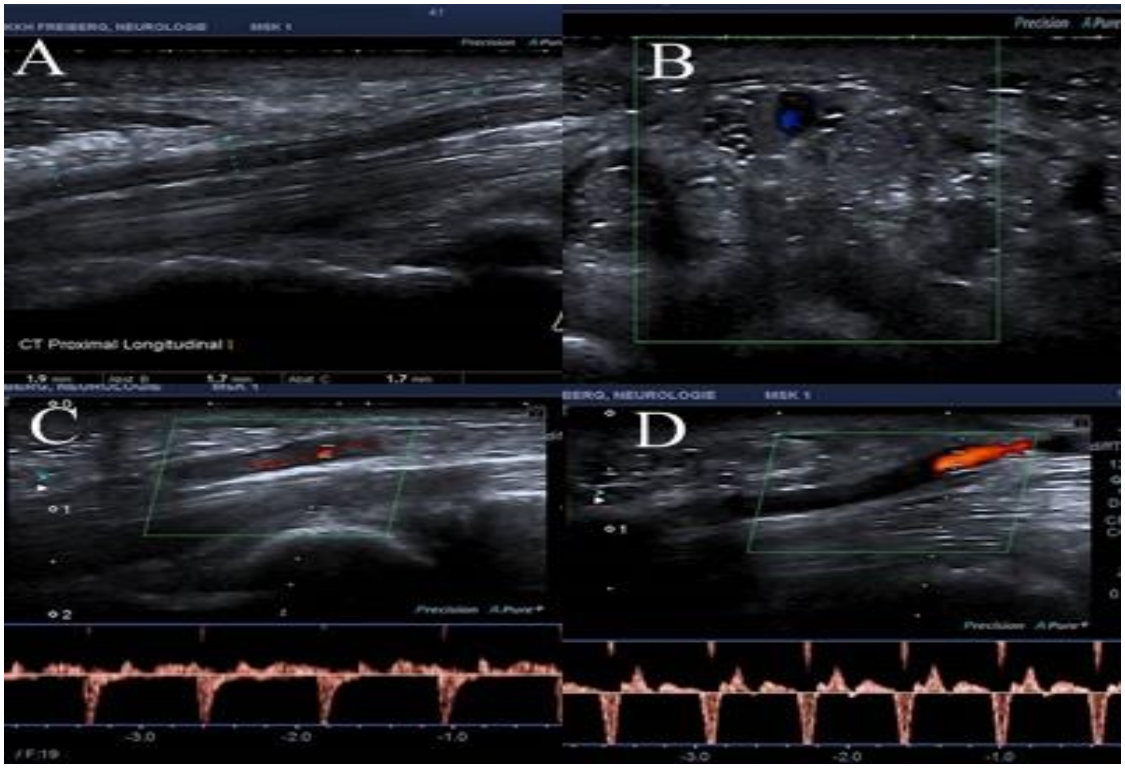

Figure 14. HRUS of the median nerve at the proximal level of the carpal tunnel. Longitudinally (A) no compression, on transverse scan enlarged median artery, only partly coloured (B). PW–mode on duplex scan showed decreased flow velocities (C) compared to the contralateral side (D) and absent flow in the middle and distal part of the persistent median artery, indicating thrombosis of the artery.

To clarify whether the thrombosed artery participated on the supply of the palmar arch, a 3 T–MRI with small hand coils was carried out, which showed the partly thrombosed vessel and sufficient collateral circulation (*Fig. 15*).

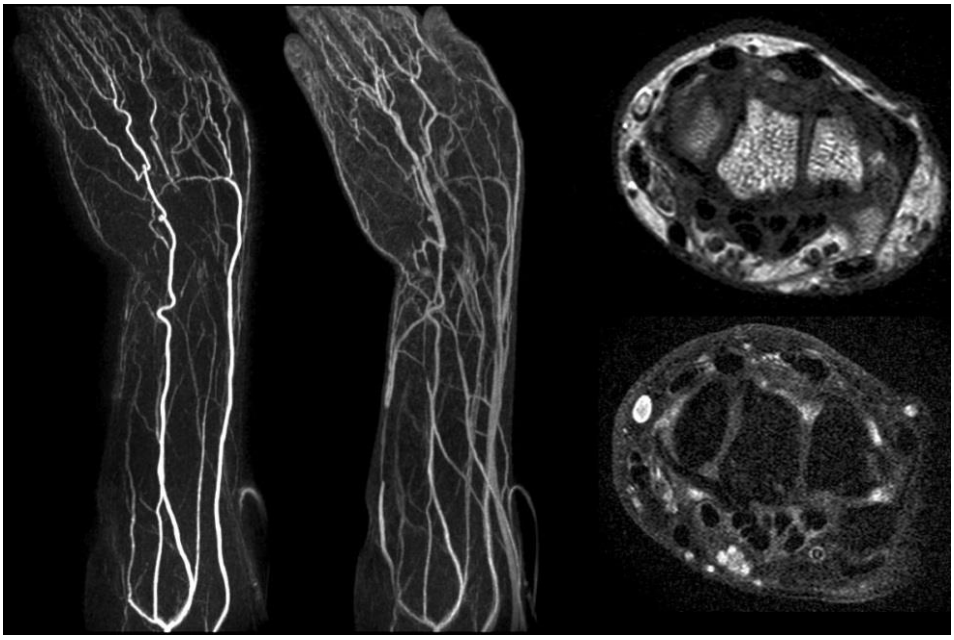

Figure 15. MR-angiography on the left side shows a thrombosis of the median artery and normal median artery on the contralateral right side. Image courtesy of Thomas Schelle (Department of Neurology, Dessau-Roßlau /Germany).

Case 2. Acute carpal tunnel syndrome after hyperventilation tetany *(31)*

A 37-year-old female patient collapsed after gastroenteritis and exposition to heat followed by hyperventilation. During the hyperventilation attack, her hand was in a flexed position for approximately 60 minutes. Immediately afterwards, she complained of hypaesthesia in the sensory area of the left median nerve. Electrophysiological assessment 8 days later showed a prolonged distal motor latency (4.8 ms) and reduction of the sensory nerve conduction velocity of the median nerve on the left side (39 m/s), consistent with carpal tunnel syndrome. On HRUS, the median nerve was slightly enlarged (*Fig. 16*) only on the left side, without segmental compression in the carpal tunnel (CSA = 0.12 cm², diameter on longitudinal scan 2.7 mm; on the right side CSA=0.08 cm², diameter 2 mm). The electrophysiologic alterations were normalized in weeks and the CSA value in 6 weeks.

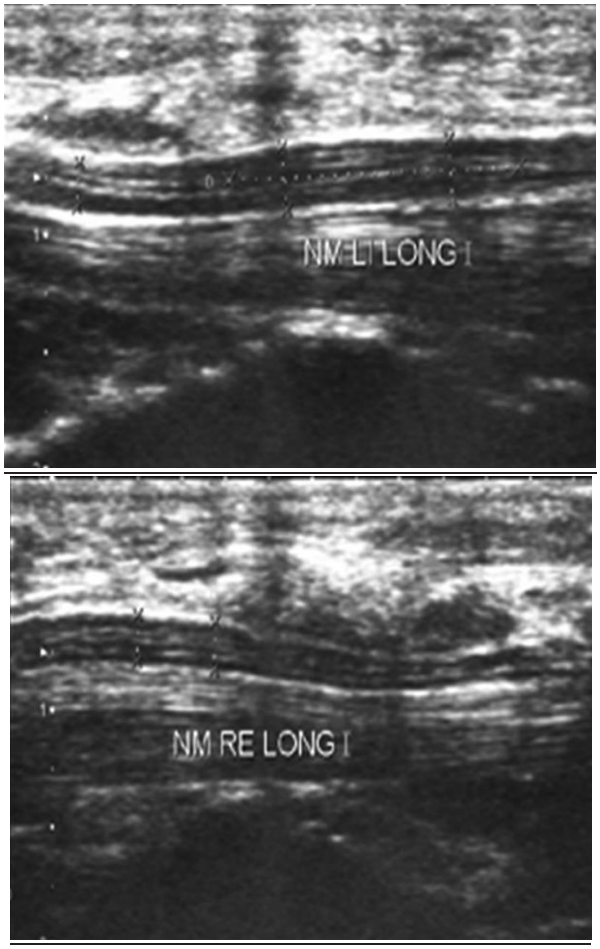

Figure 16. Acute CTS, longitudinal scan. The left median nerve is enlarged in the carpal tunnel (diameter =2.7 mm) without segmental caliber change. On the right side, normal value (diameter=2 mm).

Case 3. Schwannoma of the median nerve distal to the carpal tunnel mimicking carpal tunnel syndrome

A 53-year-old female patient complained of numbness and tingling in the three middle fingers of the left hand without pain. Electrophysiology was performed elsewhere and the results were unknown. Operation at the carpal tunnel brought no relief of her complaints. HRUS showed a normal median nerve in the carpal tunnel, but more distally a homogeneous hypoechoic ovoid mass was seen (*Fig. 17*) with hypervascularisation (not documented). The nerve entered and left the centre of the tumour. Histology confirmed the suspected diagnosis of schwannoma.

Figure 17. Homogeneous hypoechoic ovoid mass in the continuity of the median nerve distal to the carpal tunnel. Colour-duplex (not documented) has shown marked hypervascularisation of the tumour.

Case 4. Schwannoma of the median nerve proximal to the carpal tunnel mimicking carpal tunnel syndrome

A 72- year-old male patient was operated without success after complaints for more than 10 years with clinically suspected progressive carpal tunnel syndrome. He had a trauma at the distal upper arm as a young man with persistent slight sensory disturbance of the median nerve. The median nerve was normal in the carpal tunnel but more proximally, at the level of the former nerve injury more than 50 years previously, a mostly homogeneous hypoechoic fusiform mass with slight vascularisation was demonstrated (*Fig. 18*). Histology confirmed the suspected diagnosis of schwannoma with regressive changes.

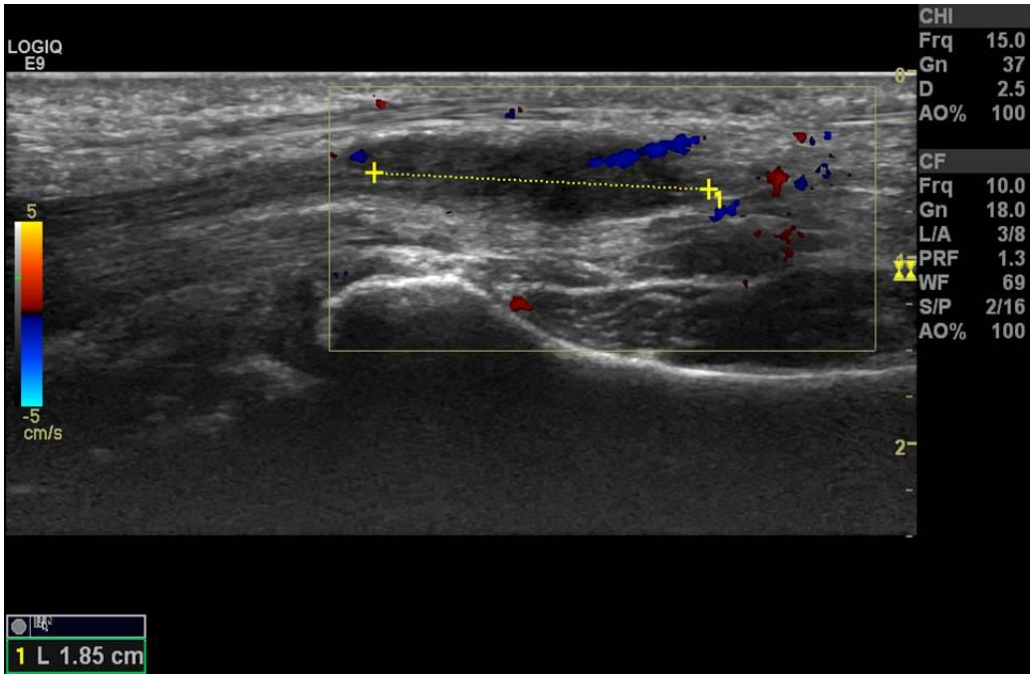

Figure 18. Homogeneous mostly hypoechoic fusiform mass in the continuity of the median nerve proximal to the carpal tunnel. Colour-duplex showed slight vascularisation of the tumour.

4.2.4. THORACIC OUTLET SYNDROME (TOS)

A 49-year-old female patient was referred to us from another hospital. She suffered for 15 years diffuse pain in the right arm, progressive paresis of the hand muscles and atrophy of the abductor pollicis brevis (APB) muscle. Electrophysiology showed slightly prolonged F-wave latency of the ulnar nerve (with normal motor nerve conduction velocity and motor action potential of the ulnar nerve), decreased sensory nerve action potential of the ulnar nerve, and absent sensory potential of the medial cutaneous antebrachii nerve. Myography showed chronic neurogenic changes only in the APB. Conventional X-ray images of the cervical spine were negative and MRI was not performed. CT scan of the cervical spine showed an enlarged transverse process of the right C7 vertebra with a rib stub and fibrous band attached to it. HRUS showed the so-called "wedge/sickle-sign": hyperechoic tip of the medial border of the scalenus medius muscle on the right side and thickened inferior trunk of the brachial plexus *(Fig. 19a* and *19b).*

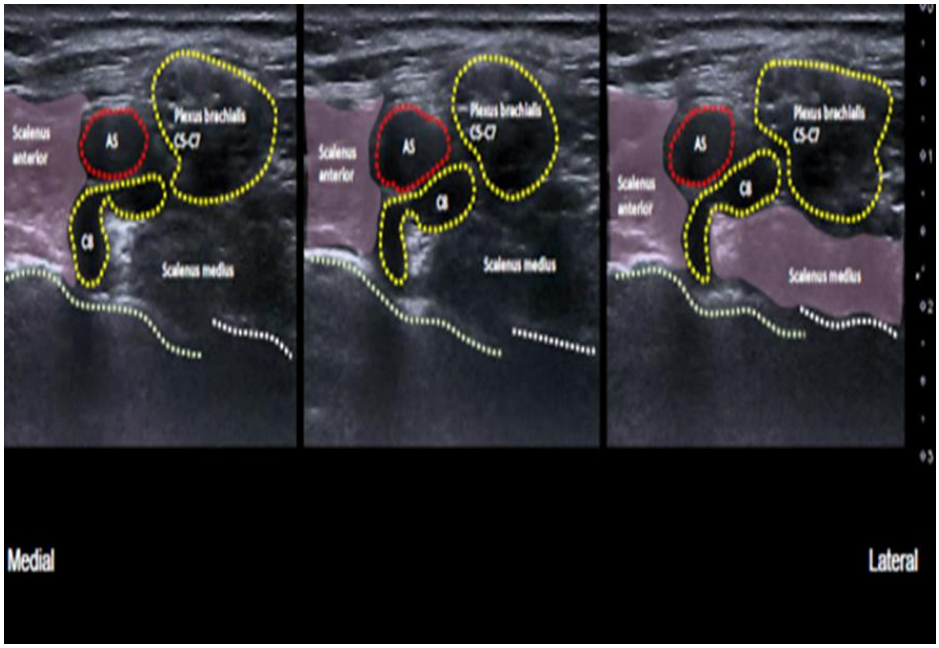

Figure 19a. HRUS showing compression of the inferior trunk (C8 root) between the scalenus medius and anterior muscles. AS= subclavian artery. Dotted lines =pleura and first rib.

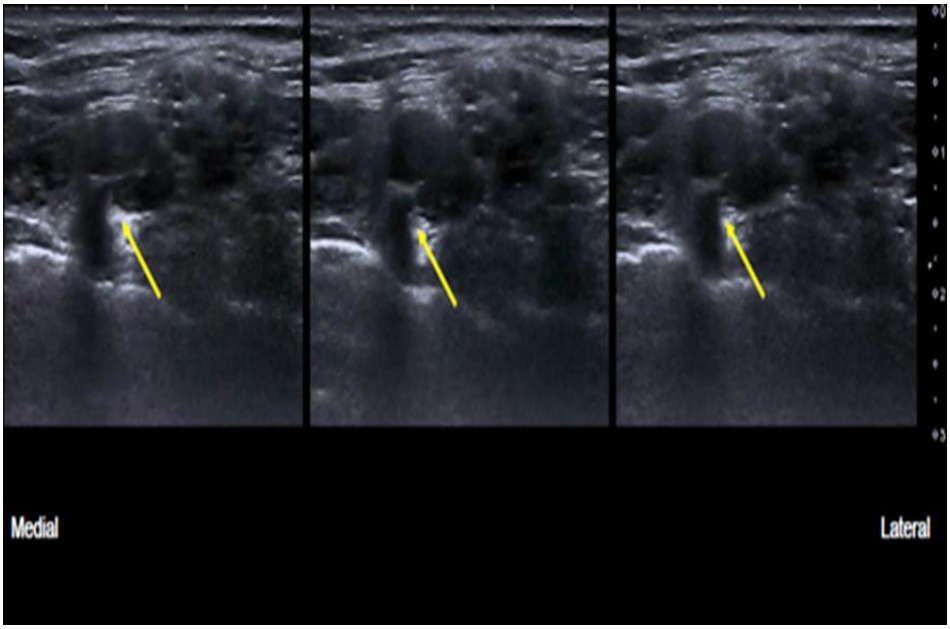

Figure 19b. HRUS showing the hyperechoic tip of the medial border of the scalenus medius muscle (arrow) causing compression of the inferior trunk (C8 root).

During surgery, compression of the inferior trunk of the brachial plexus by the medial fibrous edge of scalenus medius muscle was confirmed and resected *(Fig. 20).* Follow-up 6 months after surgery showed clinical improvement in terms of muscle power, pain and atrophy of ADM.

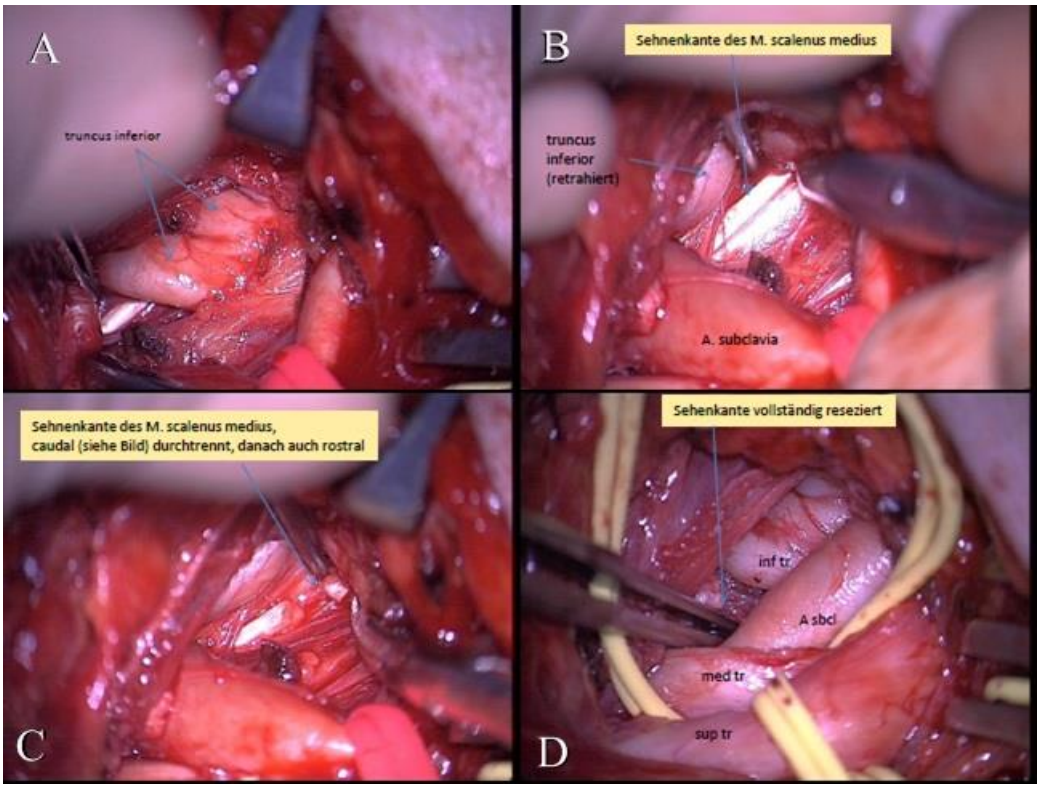

Figure 20. Intraoperative findings in TOS caused by compression of the inferior trunk (A) of the brachial plexus by the white medial fibrous edge of scalenus medius muscle (B). Partial resection of the fibrous edge (C) and total resection (D). Image courtesy of TN Lehmann, MD (Department of Neurosurgery, Bad Saarow/Germany).

4.2.5. NEURALGIC AMYOTROPHY (PARSONAGE-TURNER SYNDROME, PTS)

Case 1. Predominant radial nerve palsy in PTS

A 47-year-old female patient developed few weeks after severe shoulder pain a radial nerve palsy on the right side as a leading clinical symptom with additional minor signs of brachial plexus involvement on EMG. Electrophysiology showed isolated axonal motor (motor action potential 1.7 mV) and sensory (sensory nerve action potential 1 μV) lesion of the right radial nerve. EMG indicated involvement of the triceps brachii muscle and the more distal muscles innervated by the radial nerve. MRI

of the cervical spine was normal. HRUS demonstrated 3 months after the onset of symptoms segmental enlargement of the radial nerve from the level of the spiral groove down to the supinator tunnel, which persisted even 1.5 years after symptom onset *(Fig. 21)*. On follow–up (1.5 years later), almost complete clinical recovery was seen. In this case, the typical clinical course with sudden onset and recovery without specific treatment helped to differentiate neuralgic amyotrophy from a true focal compressive neuropathy.

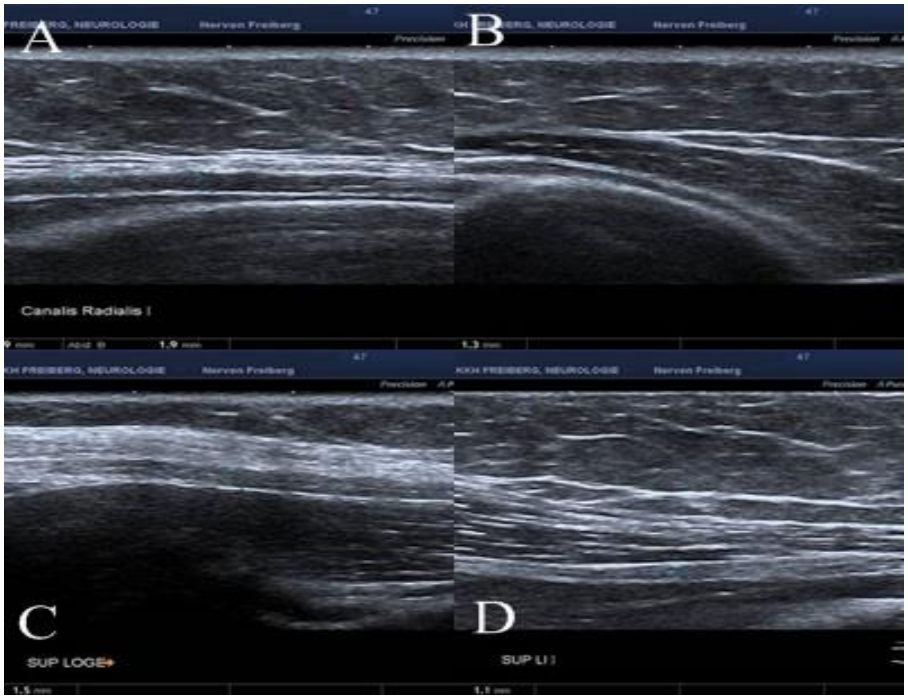

Figure 21. HRUS of the radial nerve in PTS on the right side 1.5 years after symptom onset. The radial nerve on the right side (A, C) is slightly enlarged at the spiral groove (diameter 1.9 mm vs. 1.3 mm) and the supinator tunnel (1.5 mm vs. 1.1 mm).

Case 2. Bilateral interosseus anterior nerve paresis in PTS

A 52-year-old male patient developed 2 weeks after severe bilateral shoulder pain paresis of the long flexors of the thumb and the index finger on both sides. 1.5 T MRI of the cervical spine was negative. Electrophysiology showed evidence of bilateral anterior interosseus nerve lesion. Two months after onset, HRUS demonstrated bilateral segmental enlargement of the median nerve and its fascicles at the upper arm from the mid-arm level to the elbow (*Fig. 22*). The ulnar and radial nerve and the cervical roots

C5-C7 were normal. On follow–up, 1.5 years later, almost complete clinical recovery was seen. Similar to the above mentioned first case, the typical clinical course with sudden onset, recovery without specific treatment and bilateral involvement helped in the diagnosis of neuralgic amyotrophy.

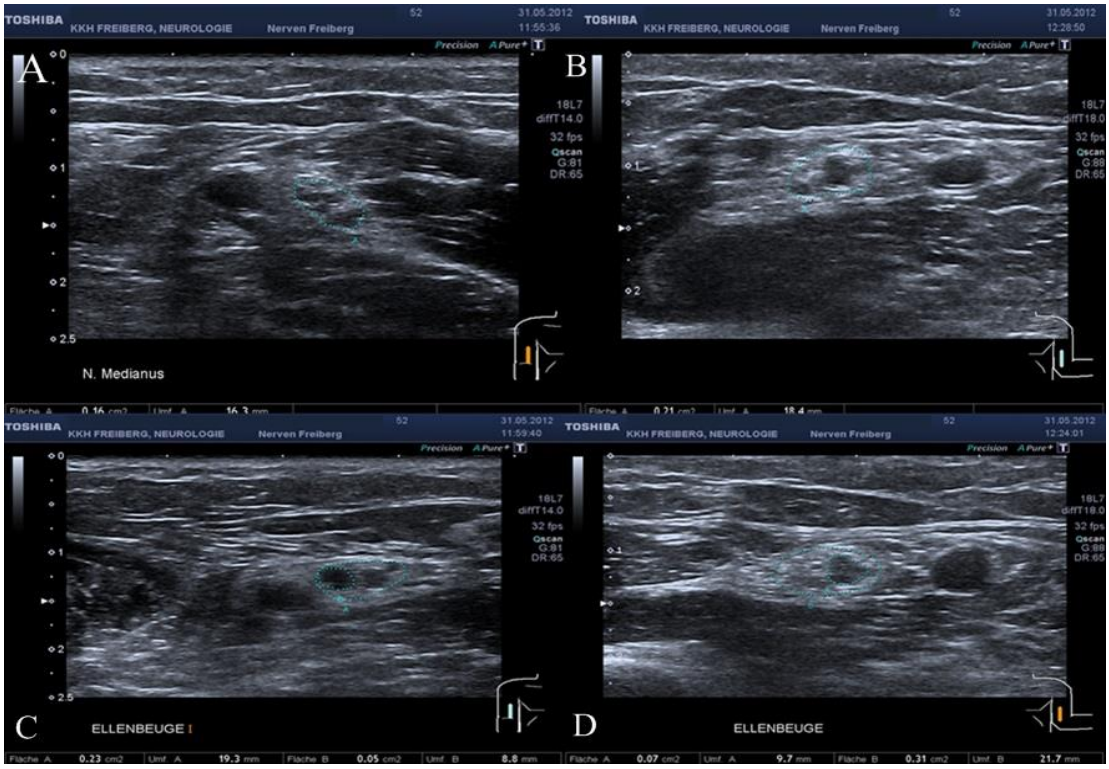

Figure 22. PTS with anterior interosseous nerve palsy on both sides. HRUS: long segmental swelling of the median nerve and its fascicles at the upper arm from the mid-arm level to the elbow. CSA of single fascicles 0.05-0.07 cm², CSA on the right side from proximal (mid-arm) 0.16 cm² (A) to distal (elbow) 0.23 cm² (C) , resp. on the left side 0.21 cm² (mid-arm) (B)and 0.31 cm² (elbow) (D).

4.2.6. RARE POLYNEUROPATHIES

Case 1. Paraneoplastic multiple mononeuropathy *(32)*

A 58-year-old male patient, who worked as a master bricklayer and with a history of cigarette smoking (50 pack-years), presented with a 1.5-year history of slowly progressive, asymmetric, especially right-sided numbness of the 1-3rd fingers on both sides and a 1-year history of numbness of the 4-5th fingers on the left side. Strength and

muscle volume of his left hand slowly diminished. One year before presentation, he was operated for suspected right carpal tunnel syndrome, but without subjective benefit. Later numbness of the left 4th and 5th fingers, as well as diminished strength in abduction of left 5th finger developed. Entrapment neuropathy of the left ulnar nerve at the elbow was suspected and operated by anterior transposition of the nerve. In addition, the right carpal tunnel was surgically revisited. Symptoms persisted and eventually increased. On examination, severe neuropathy of the left ulnar and moderate neuropathy of the right median nerves were found. Specifically, severe paresis of left ulnar-innervated hand muscles (MRC grade 2) and slight paresis of the right thumb abduction (MRC grade 4) were observed. The strength of other muscles and lower extremities was normal. Left ulnar-innervated hand muscles were atrophic, and the hand had a claw appearance. Hypaesthesia to light touch was present in left 4-5th fingers, the ulnar aspect of the hand and forearm, the lateral upper arm, the volar side of the right 1-3rd fingers, as well as the lateral side of the lower right leg. Electrodiagnostic studies from both median nerves showed axonal sensory–motor neuropathy without conduction block, and ulnar nerve conduction studies showed severe, left, non-localizing axonal motor–sensory neuropathy and neuropathy of left ulnar nerve at the elbow. Electromyography showed fibrillation potentials and neurogenic changes in ulnar-innervated muscles in the left hand. Electrophysiological studies of the lower extremities were normal. HRUS showed focal enlargement and hypoechogenicity of the left ulnar nerve in the entire upper arm, focal enlargement, and hypoechogenicity of left median nerve at the elbow over a 10 cm-long segment (*Fig. 23*). Multiple entrapment neuropathies could therefore be ruled out, and multiple mononeuropathy with focal nerve hypertrophy was diagnosed.

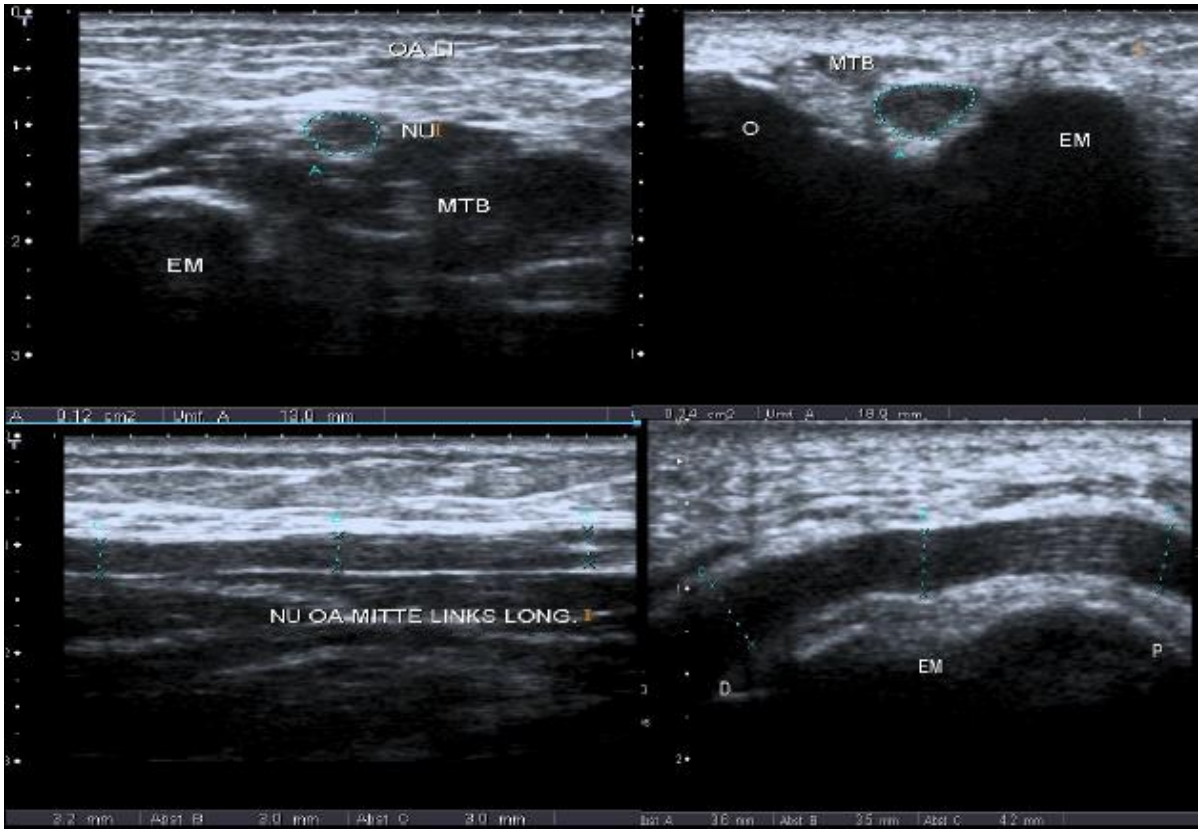

Figure 23. HRUS of the left ulnar nerve in paraneoplastic multiple mononeuropathy. The nerve at the elbow (CSA 0.24 cm², diameter 3.5 mm) and at the upper arm (CSA=0.12 cm², diameter 2.2 mm) is hypoechoic and enlarged.

Extensive work-up demonstrated only slightly elevated cerebrospinal fluid protein (607 mg/L, normal <500 mg/L). All other parameters (including tests for syphilis, borreliosis, thyroid function, porphyria, Refsum disease, sarcoidosis, vasculitis, collagenosis, and vitamins B1, B6, B12, E, and folate deficiencies) were normal. Testing for paraneoplastic serum antibodies revealed high titers of anti-Hu antibodies on immunofluorescence testing on primate cerebellum and intestine. Immunoblot with recombinant antigen confirmed specificity. No other paraneoplastic antibodies were positive. CT confirmed the suspected lung cancer. Biopsy histologically revealed small-cell lung cancer.

Case 2. MADSAM polyneuropathy

A 65-year-old male patient had a 10-year-long history of slowly progressive asymmetric paresis with atrophy, predominantly on the upper arm without sensory

disturbance. GM1-antibodies were positive, cerebrospinal fluid findings were normal. Electrophysiology showed severe, asymmetric motor axonal damage without localizing findings. In another hospital, amyotrophic lateral sclerosis was supposed and the patient was referred for HRUS. HRUS showed markedly enlarged nerves of the upper arms on both sides, predominantly on the most involved side with marked changes of the fascicle calibers and of the cervical roots bilaterally (*Fig. 24*).

Figure 24. HRUS in MADSAM. Enlarged (diameter: 5.3 mm) median nerve at the upper arm (right side) with caliber change of the fascicles.

Case 3. Polyneuropathy in vasculitis

A 72-year-old male patient had for 3 months generalised arthralgia, for 3 months burning feet sensation more on the right side and violet-red skin changes on the lower leg and on the back of the foot. Laboratory values showed thrombocythaemia (128 G/l), decreased red blood cell count (3.9 T/l; N > 4.6 T/l), in differential blood cell count 54% lymphocytes, slightly elevated C-reactive protein (8.8 mg/L), and markedly elevated rheumatoid factor 436 IU/l (N<15). ANA, pANCA and cANCA were negative. Electrophysiology showed an axonal distal-symmetric motor and sensory neuropathy. HRUS demonstrated the isolated enlargement of the tibial nerve (*Fig. 25*). Histologic

examination of the sural nerve revealed leukocytoclastic vasculitis. Further rheumatologic assessment showed Sjögren syndrome and parotid biopsy confirmed chronic B-cell lymphoid leukaemia.

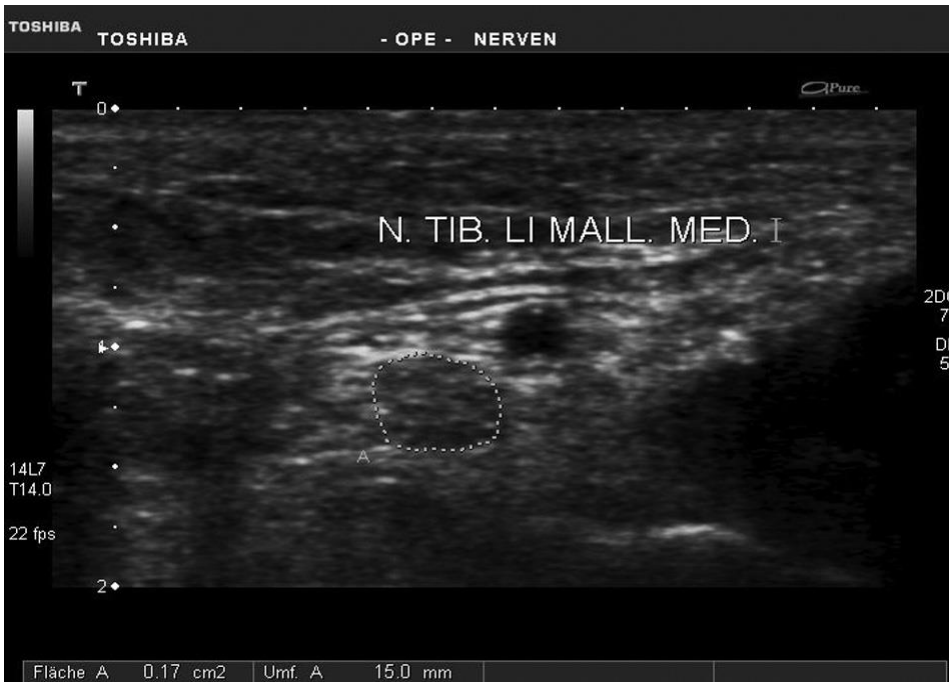

Figure 25. HRUS of the left ankle. The CSA of the tibial nerve is enlarged (0.17 cm²).

5. DISCUSSION

5.1. Normal values and reliability assessments

High resolution ultrasonography has become an effective tool for the investigation of peripheral nerve disorders. It has been demonstrated that peripheral nerve pathology results in focal or diffuse thickening of the nerves together with a pathological change of echostructure and echogenicity (2). Examination of pathologic peripheral nerve in HRUS is based mainly on changes in nerve size, and in clinical practice the contralateral side is often used as an internal control. The most common method used to quantify nerve size is the measurement of the cross-sectional area (CSA) of the nerve.

The increase of CSA of the involved nerve allows precise localization in entrapment neuropathies and peripheral nerve tumours (27). Moreover, enlargements of multiple nerves in acquired and hereditary polyneuropathies are also described (19) Therefore, it is essential to compare nerve size parameters measured in patients to reference values. However, reference values are still lacking for some nerves and those published tend to show variability probably due to factors such as measurement accuracy, expertise of the examiner, equipment, location of the nerve, and patient specific factors (ethnicity, age, gender, body mass, height). Our aim was to contribute a large set of reference values to the pool of normative data currently being amassed in the literature by measuring the cross sectional areas of 10 upper and lower limb nerves at altogether 14 sites in 56 healthy individuals. Other studies usually assessed fewer nerve segments (*Table 4*). In more recently published studies in 2013, nerves were measured bilaterally and not only unilaterally at more sites (26) but only at the upper extremity (22) and at 15 sites bilaterally (33), but partly at different segments (no measurement at the mid upper arm level, instead of that at the axilla and no measurement of the cervical roots C5-C7).

Our study subjects represented a broad range of age and a balanced gender distribution from two different European countries, but ethnicity (Central-European Caucasian) was homogeneous. Although sample size could be larger, the narrow range of 95% confidence intervals for the mean, the relatively low coefficient of variation (generally between 20-30%) (*Table 3)* and the normal distribution of values of a given nerve, gender groups examined separately or combined and with different resolutions (analysis not shown), all support that the sample size of our study is acceptable. Furthermore, no significant differences were found when comparing two independent cohorts (i.e. German and Hungarian populations), which also supports the validity of collected normal values. We found no consistent correlations between CSA values and age, height, or body weight, but males had significantly larger values than females for nerve segments in the upper arm. Regarding the age dependent correlations, our study had some limitations. Due to only 56 examined mostly middle-aged subjects, the correlations could not been investigated in sufficient numbers in young and old subjects. Likewise, these different age subgroups could not be compared.

Our findings are similar to some earlier reports but data in the literature are not fully consistent in this respect. Similarly to our results, Heinemeyer et al. found no correlation between nerve size parameters and age, height and body weight, but reported thicker nerves on the upper limbs in males (34). Cartwright et al. (18) reported that nerve size correlated with body weight and body mass index, and that these correlations were most pronounced in the nerves of the proximal leg. They also found that females had smaller nerves than males. No difference in nerve size parameters was found when dominant and non-dominant sides were compared. According to Zaidman et al., CSAs of the ulnar and median nerves are larger with increasing height, at proximal sites and at sites of entrapment, but are independent of age and no side difference was observed (19). Kerasnoudis et al. (33) found independence to height and weight in most of the peripheral nerves. Significant differences with regard to sex were found only in the ulnar nerve in Guyon's canal, peroneal nerve at the popliteal fossa and sural nerves. Only the median nerve in the axilla and the radial nerve in the spiral groove showed a statistical significant decrease with advancing age and on the other side, significant higher cross sectional area values showed the tibial nerve (ankle) with advancing age. Despite the fact that our CSA reference values for cervical roots and at the upper extremity were almost identical to those of Won et al. (35) (*Table 4*), their CSA values correlated by contrast significantly with weight, body mass index, height, and gender. In a Japanese study (36), where only the median nerve and the ulnar nerve at the upper extremity were examined with CSA measurements, gender, height and wrist circumference were determined to be dependent factors for all evaluation sites and non-entrapment sites along the median nerve. Only wrist circumference was determined to be dependent factor for all evaluation sites along the ulnar nerve. Nerve sizes were larger in male participants at 3 of 5 measurement sites both for the median and the ulnar nerve. Significant BMI-based and age-based differences in nerve size were present only at 1 measurement site of the median nerve. Height-based differences in reference nerve sizes were present at 3/5 sites of the median nerve. Because in that study cervical roots were examined longitudinally without CSA measurements, comparisons with our study are not feasible.

Table 4. Mean (±SD) peripheral nerve CSA values (mm^2) in our study and values published to date

Nerve/Site	Present study n=56	Cartwright et al. 2008 n=60	Zaidman et al. 2009 n=100	Haun et al. 2010 n=33	Tagliafico et al. 2012 n=60	Won et al. 2012, 2013 n=97	Kerasnoudis et al. 2013 n=75	Sugimoto et al. 2013 n=60
C7	10.0±2.9	6.3±2.4		12.1±4.1		10.43 ± 1.86		
C6	9.5±2.7	(combined mean value of the three trunks)		10.6±4.3		8.98 ± 1.65		
C5	5.6±1.6			7.1±4.1		5.66 ± 1.02		
Median arm	8.9±1.8	8.9±2.1	8.9±2.0			9.4±1.4 (R)	8.4 ±2.87	8.2 ±1.7
Ulnar arm	6.3±1.7		6.2±1.4			5.9±1.1 (R)	6.53 ±1.82	4.8 ±1.0
Radial arm	4.2±1.0	7.9±2.7				4.6±0.9 (R)	3.26 ±1.52	
Ulnar epicond	7.6±2.1		7.3±1.7			7.2±1.4 (R)	5.33 ±1.4	6.7 ±1.9
Median forearm	5.7±1.3	7.5±1.6	7.9±2.4			6.5±1.1 (R)	6.6 ±1.6	6.0 ±1.3
Ulnar forearm	5.2±1.3		5.5±1.4			6.3±1.0 (R)	5.46± 1.26	4.7 ±1.0
Spf radial forearm	2.3±0.7					2.0±0.5 (R)**		
Median carpal	8.5±1.8	9.8±2.4	9.7±1.9			8.3±1.5 (R)	8.43 ±2.07	8.5 1.7
Peroneal	8.9±2.0	11.2±3.3			13.2±14*		7.1 ±2.3	
Tibial	9.6±2.2	13.7±4.3			9.6±4*		6.36 ±1.45	
Sural	1.8±0.6	5.3±1.8 (at the distal calf)			3.6±11* (at the distal calf)		1.82 ±0.64	

CSA=cross-sectional area; Spf=superficial; SD=standard deviation; *mean values are provided with standard error of measurement; R=right side; **measured at the elbow

Table 4 shows, together with our results, some of the most important studies that published normative values for CSA of peripheral nerves. Among these studies, our study is the first to evaluate most of the important nerves on the upper and lower limbs in the same person, including pure sensory nerves and cervical roots in a healthy Central-European population. Kerasnoudis et al. (33) performed their study later as we have done it, but published earlier the data and they did not made CSA measurements of the cervical roots.

The CSA of most nerves, as in our study, ranges from 2 to 10 mm^2. However, we did not measure femoral and sciatic nerves, which are considerably larger, with CSA as high as 41 mm^2 in case of the sciatic nerve (21). *Table 4* also shows that CSA values across these studies are consistent for the major upper limb nerves, with the exception of the radial nerve in the spiral groove reported by Cartwright et al. (18). However, in the most recent studies of Won et al. (22) and Kerasnoudis et al. (33), the radial nerve values reported by Cartwright et al. can be considered as an 'outlier', probably due to methodological reasons. Concerning the superficial radial nerve at the distal forearm, the few studies available (22, 23) published CSA values of 2-3 mm^2, similarly to ours. The ultrasonographic visualization and measurement of the cervical roots of the brachial plexus are limited by the deep position and oblique course of the roots and also by body habitus, accurate measurement becoming sometimes impossible. However, there is a good correlation of our results with those previously reported by Haun et al. (20) and recently presented by Won et al. (35).

Our data are consistent in that the C5 root is the smallest among the cervical roots, followed by the C6 root and the C7 root being the largest. In the median and ulnar nerve we found site-based differences of the CSA along the course of the nerve. Nerve size of the median nerve decreased from the carpal tunnel to the distal forearm and increased at the mid-arm site. The smallest nerve sizes of the ulnar nerve were at the forearm, the largest nerve sizes were at the elbow and the size decreased again proximally at the mid-arm level. Our findings are consistent with the results of the other groups (*Table 4*). Neither anatomic nor histologic research has ever considered site-based differences along peripheral nerves. Additional research is necessary to confirm this findings from the viewpoints of anatomy and histology (36).

Tagliafico et al. (21) emphasizes that the deep position of the nerve affects measurement accuracy due to poorer visualization. They have found that the minimum detectable difference for between-limb comparisons for the sciatic nerve, especially in at his deep site at the piriformis level, is much higher than that of superficial nerves, mainly explained by the poorer visualization. Concerning lower limb nerves, variability appears to be higher. In the study of Tagliafico concerning side-to-side comparison of lower limb nerves, they found that the standard error of measurement and minimum detectable side-to-side difference are relatively high for the peroneal nerve at the fibular head (CSA difference 5.1 mm^2) and the tibial nerve at the tarsal tunnel (2.2 mm^2) and less for the sural nerve (1.4 mm^2) (among the nerves also examined in our study). It is a general experience of those performing ultrasonography of peripheral nerves that - due to the echogenic properties of surrounding tissues - lower limbs nerves are less clearly demarcated and thus their borders, especially on cross-sectional images, may be difficult to discern. This of course accounts for measurement inaccuracy. Furthermore, the peroneal nerve has an oblique course around the fibular head and even slight tilting of the probe may affect nerve size measurements on cross-sectional scans. The sural nerve measurements in our study are non-comparable with Cartwright et al. (18) and Tagliafico et al. (21), because we made measurements at the proximal calf rather than at the distal calf. Kerasnoudis et al. (33), who performed the measurement at the same site at the proximal calf, had similar results to ours. Overall, side-to-side differences were not statistically significant at any level in the lower limb nerves. Therefore it was concluded that in general the healthy contralateral side can be used as an internal control[21].

Fryback and Thornbury (38) described a hierarchal model with 6 levels for assessing the efficacy of diagnostic imaging modalities, and the first level is the need to demonstrate that the technique is valid and reliable.

Inter-rater reliability was analysed in several reports, however, the intraclass correlation coefficient (ICC) in our study was high (0.98) when compared to previous studies. Impink et al. found only a moderate reliability in measuring the parameters of the median nerve (39). Cronbach's alpha ranged from 0.754 to 0.940 for the interobserver reliability, when the CSA of the median nerve was measured at the entrance of the carpal tunnel and 2 cm proximal to the palmar wrist crease (40). Other

authors reported mostly good or excellent results but had lower ICC values than calculated in our study (18-19, 41). This may be explained by the fact that our two investigators have been working close together for several weeks in the training session, and measurements were taken using precisely predefined anatomical landmarks.

Reliability assessments have been performed as well in the ultrasound-based evaluation of the optic nerve sheath diameter (ONSD) for detecting raised intracranial pressure. In a study to establish normal values and to assess reliability measurements, the ONSD of 40 healthy subjects was independently measured by 2 investigators. The mean ONSD was 5.4 ±0.6 mm. Pearson's correlation coefficient between the 2 investigators was 0.81 on the right side and 0.84 on the left (42). Other ultrasound-based studies dealing with this issue also showed high consistency (43-45). The results resemble those published on interobserver variability in ONSD assessment deriving from 2 MRI studies (46-47).

Intra-rater reliability has been rarely reported in peripheral nerve ultrasound measurements (22-23). We analysed 14 measurements of 6 patients repeated by the same investigator one day apart. The high ICC value (0.93) reflects excellent reliability and reproducibility of neurosonography in the hand of an experienced and well-trained examiner. Other authors reported high concordance as well, but mostly the median nerve was examined, whereas several nerves of the upper and lower limbs and cervical roots were measured in our study, including nerves that are more difficult to examine. Cronbach's alpha was reported to range from 0.924 to 0.996 for the intraobserver reliability when the CSA of the median nerve was measured at the entrance of the carpal tunnel and 2 cm proximal to the palmar wrist crease (40).

The ultrasound-based evaluation of the optic nerve sheath diameter showed also high intra-observer reliability (42) (Cronbach's Alpha was 0.95 for the right bulbus and 0.97 for the left).

A novel and noteworthy element of our study is the evaluation of *inter-equipment reliability*. Similarly to the intra-rater reliability, it was also a 'test-retest' assessment carried out by the same investigator but on two different devices, with linear array transducers of different frequencies (Philips vs. Toshiba, 15 MHz vs. 12 MHz transducers). Statistical analysis showed a high overall concordance (ICC=0.86), suggesting a good reproducibility of measurements carried out on different ultrasound

equipments. The difference between the resolution of a 12 MHz and a 15 MHz transducer did not prove to be significant with respect to nerve size measurements. Only a single study was found in the literature, which reported good concordance of median nerve measurements performed in different laboratories (41), but inter-equipment reliability has not been studied previously involving the same investigator and the same patients on multiple nerves.

Validity and reliability of nerve and muscle ultrasound were assessed systematically in a recent study (48). CSA (and muscle thickness) were measured ultrasonographically at several sites in 4 cadavers, which were then dissected, and actual measurements were obtained. Intra-rater and inter-rater reliability, between 3 and 5 ultrasonographers, with varying experience levels, were assessed later on healthy volunteers. Correlation coefficients for nerve and muscle validity were >0.968 ($P<0.001$), and for intra-rater reliability were >0.901 ($P < 0.001$) for still and real-time images. Correlation coefficients for inter-rater reliability were more varied, but for still images they were all significant at the $P<0.001$ (0.542–0.998) level. Similarly to our results, the authors concluded that overall nerve and muscle ultrasound is a valid and reliable diagnostic imaging technique (48).

In conclusion, the *good reliability and reproducibility* of neurosonography in the examination of peripheral nerve disorders in the hand of experienced investigators is highlighted by our study. The use of predefined anatomical landmarks is essential to obtain comparable data. The excellent reliability of our measurements serves as a basis for the acceptance of the normal values provided by our study. Nonetheless, it is important to note that ultrasonographic measurements of peripheral nerves should be put in context of clinical and electrophysiological data, and caution is advised when interpreting minor deviation from normative data. For future ultrasound studies involving pathologic nerves, caution is advised concerning the difficulty of differentiating between normal and pathological heterogeneity of cross sectional area variation in peripheral nerves, especially in the case of immune-mediated neuropathies. Recently, three novel ultrasound measures have been introduced, aiming to quantify cross- sectional area changes of peripheral nerves and to differentiate focal from diffuse nerve enlargement: the ‘‘intranerve cross-sectional area variability’’ (for each nerve) (49), defined as the ratio of maximal cross-sectional area / minimal cross sectional area,

the ‘‘internerve cross-sectional area variability’’ (for each subject), defined as the ratio of maximal intranerve cross-sectional area variability / minimal intranerve cross-sectional area variability, and the ‘‘side to side difference ratio of the intranerve cross-sectional area variability’’ (for each nerve), defined as the ratio of the side with maximal intranerve cross- sectional area variability / the side with minimal intranerve cross-sectional area variability (50).

5.2. Ultrasonography of patients with rare neuropathies

Several rare neuropathies with different aetiologies were examined by HRUS. Reports on the sonographic findings in rare entities such as sarcoidosis (51), extramedullary affection of the peripheral nerve due to a plasmacytoma (52-53), and intraneural metastasis (54) have been described by others. Rare nerve tumours and focal tumour-like lesions may cause particular differential diagnostic difficulties, such as our own cases: amyloidosis, primary intraneural lymphoma and plexiform growth variant of neurofibromatosis.

5.2.1. RARE TUMOURS AND FOCAL TUMOUR-LIKE LESIONS

Concerning *amyloidosis*, 27 amyloidogenic proteins are known to be associated with human diseases. For a detailed overview on clinical features, diagnosis, and therapy of the condition, see the literature (55). The main presentation of AL-amyloidosis is generalized distal symmetrical sensory-motor neuropathy. In a patient with AL-amyloidosis neuropathy, electrophysiologically characterized by a pure axonal loss, high resolution ultrasound could demonstrate a generalized thickening of the peripheral nerves, caused by an increasing number of the identifiable fascicles, but with no specific pattern of these changes (56). Focal mononeuropathy, especially of the upper limbs, is an uncommon presentation of primary amyloidosis and was confirmed by nerve biopsy (AL, light chain amyloidosis) in one case (57). On the other hand, only a few focal tumour-like lesions in some peripheral nerves of lower extremities or cranial nerves due to amyloidosis have been described in the literature so far. Amyloidoma of

the sciatic nerve and the potential value of highfield-MR for detection was reported (58). In another paper, in two cases the amyloidoma caused focal lesions in the lumbosacral roots and plexus (59). Interestingly, almost all amyloidomas of the peripheral or cranial nerves were organ restricted neoplasms, unrelated to systemic amyloidosis and of the AL-lambda type. On MRI, gadolinium-uptake without significant surrounding tumour-oedema was seen. Serum amyloid protein A, transthyretin and beta-2 microglobulin could not be detected. Unlike some forms of systemic amyloidosis the course of a focal amyloidoma within the peripheral or cranial nerves seems to be rather indolent and is reminiscent of the biologic behaviour of lymphoma of mucosa-associated lymphoid tissue – MALT – (60).

Secondary amyloidosis (AA) is seen in patients with rheumatoid arthritis and other chronic inflammatory diseases, and is associated with the accumulation of protein A. The presence of slightly elevated antibodies against amyloid-A in the serum in the presented case would be indicative of a possible secondary amyloidosis but no disease associated with amyloidosis was confirmed. To my knowledge, this is the first reported case of an isolated radial nerve mononeuropathy with no systemic features caused by amyloidosis and assessed by HRUS. Thus, amyloidosis should be included in the differential diagnosis of rare non-traumatic radial nerve lesions.

Primary lymphomas of peripheral nerves are extremely rare, with the bulk of the literature being case reports. The nerve most commonly affected is the sciatic nerve, with 11 cases reported, of which 10 cases were B-cell-lymphomas and only 1 case T-cell-lymphoma (61). Electrophysiology shows axonal lesion, and the course is progressive. One case with isolated occurrence in the radial nerve was reported (62). HRUS of the lymphoma in the described case report in the ulnar nerve showed common features to the case described in the sciatic nerve (61). It had some inhomogeneous inner echos and good vascularisation, based on which a so-called “ancient schwannoma” with regressive changes would have been a plausible diagnosis. In both cases further manifestations of the lymphoma have been seen, in our case in the flexor carpi ulnaris muscle and in the case with the sciatic nerve in the intrapelvic, dorsal gluteal and femoral nerves as well. In our case, the very long segment of the nerve involvement from the axilla until the elbow, and the somewhat irregular contour spoke against a schwannoma. However, in a recent report it has been shown that a

differentiation between schwannoma, neurofibroma using high resolution ultrasound is not possible and histologic confirmation is needed in sonographically suspected tumours (63).

Regarding nerve lesion in *rheumatoid arthritis*, in 30 cases of rheumatoid arthritis with neuropathy, five patterns of neurological involvement were described. Lesions of major peripheral nerves on the upper arm were present in ten of those cases. Only one patient had a lesion of the posterior interosseous nerve due to an effusion in the elbow-joint (64). Posterior interosseous nerve (PIN) palsy is a very rare complication of rheumatoid arthritis affecting the elbow joint. Eighteen cases of PIN palsy due to rheumatoid arthritis have been reported (65). Elbow joint swelling and compression of the PIN at the arcade of Frohse (proximal edge of the superficial head of the supinator muscle) are the main causes for PIN entrapment in rheumatoid arthritis. Vasculitis or drug toxicity may be additional causes. In our case, HRUS identified an atypical site of the lesion, at the distal end of the spiral groove, which was consistent with the results of the electrophysiological study. Active synovitis of the right elbow or features of vasculitis were not seen.

The most common benign peripheral nerve sheath tumours are *schwannoma* and *neurofibroma* (5.2% and 5.3% of all benign soft tissue tumours, respectively) (66). Neurofibromas have a homogeneous hypoechoic echotexture with mostly low or no vascularization. The typical sonographical presentation of solid schwannomas or neurofibromas is characterized by a peripheral nerve that centrically or eccentrically enters and exits a more or less homogeneous hypoechoic ovoid or fusiform mass that has well defined margins and shows posterior acoustic enhancement. In larger solitary neurofibromas and schwannomas, good vascularization may be observed with the aid of colour Doppler.

The sonographic differentiation between plexiform type tumours and tumour-like lesions or focal manifestation of immune-neuropathies is challenging. All of these focal lesions may present as focal fusiform enlargement of the nerve and a hypertrophic-hypoechoic remodelling of its fascicles. In case of a plexiform neurofibroma, if present, the history of a neurocutaneous syndrome (neurofibromatosis type I) helps, whereas in inflammatory neuropathies clinical, subclinical (in electrophysiology) and sonographic involvement of other nerves may help. Finally,

nerves tumours show more pronounced contrast agent uptake in the MR-neurography. But in most cases, only biopsy of a nerve fascicle leads to definitive diagnosis. In our case, HRUS helped to show the exact localization of the tumour in a difficult examination site of the radial nerve between the axilla and spiral groove. Furthermore, HRUS allowed the exact localization of the tumour, which was more proximal than expected by EMG results.

5.2.2. NERVE TORSION

Peripheral nerve palsies of the upper extremity caused by non-traumatic *nerve fascicle torsion* are rare. The first descriptions of this condition date from 1966 (67) and 1970 (68). Nerve torsion can involve all fascicles or only single fascicles of the nerve. In one patient with a median nerve lesion a total of 24 hourglass-like constrictions along four nerve fascicles were described (69). The anterior and posterior interosseous nerves are the most frequently involved. In a recent review of torsion neuropathies on the upper arm, only one case of radial nerve involvement was described, and surprisingly more proximal torsions were found involving the axillary nerve, musculocutaneous nerve and the suprascapular nerve (70). Both traumatic and spontaneous torsions have been described. The aetiology of this disorder is unclear. The aetiology of nerve fascicle torsional lesions might involve an inflammatory response to infection or an autoimmune response (71). Other authors (72) assumed that isolated neuritis with inflammation in the nerve fascicles of upper extremity resulted in oedema of the nerve fascicles and later local fixation could be the main factor in forming constrictions. Local irritation or subclinical trauma leading to inflammation results in local oedema, impaired nerve gliding, vascular compromise, and initiation of a vicious circle causing a substantial increase in endoneurial fluid pressure and secondary intrafascicular oedema (73). A mechanical hypothesis for the constriction of the anterior interosseous nerve in the narrow canal between the forearm muscles was provided by other authors (74). In a recent Chinese study (75), all nerve torsions in 11 patients were monofascicular and the radial nerve was involved in 10 patients and the ulnar nerve was involved only in one patient. Pathological sections of the patients in the Chinese study showed oedema and inflammatory cell infiltration of the nerve fascicle, which was accordant with the theory

of an inflammatory response by Hosi and Lundborg (74,76). The oedema of the fascicles and consequent local fixation as the main factor in forming constrictions were consistent with the findings at surgery. Idiopathic radial nerve constriction proximal to the elbow after the nerve pierced the lateral intermuscular septum was first described by sonography, characterized by an hourglass-shaped appearance and a thickening of the nerve proximal and distal to the constriction. At surgery one month after the sonography, the hourglass-shape of the nerve lesion was confirmed without description of a torsion and the aetiology remained unknown (76). The sonographic characteristics of torsion include an hourglass-shape appearance in the region of nerve fascicle torsion, hypoechoic fascicles in the affected segment and thickening of the diameter caused by oedema (52). MRI combined with DW-MRN was also an effective diagnostic step in the evaluation of patients with suspected nerve fascicles torsion (52). In our case with involvement of the radial nerve at the upper arm, torsion was subsequently confirmed by intraoperative and histological findings. 1.5 T-MRI was negative and the diagnosis was confirmed by surgery and by histology. It is important to note that the twisting and constriction of the radial nerve was seen only after the removal of the adventitia. If an hourglass-shaped appearance of the nerve, with thickening of the nerve proximal and distal to the constriction is seen, torsion neuropathy should be suspected as possible differential diagnosis of PTS.

5.2.3. RARE DISEASES MIMICKING CARPAL TUNNEL SYNDROME

Idiopathic *carpal tunnel syndrome* is a common condition where the value of electrophysiology in the confirmation of the diagnosis is well known, but there are some *rare entities*, which may also cause carpal tunnel syndrome. HRUS measurement (77) of median nerve cross-sectional area at the wrist is also accurate and may be offered as a diagnostic test for carpal tunnel syndrome (Level A). Based on Class II evidence, HRUS of the wrist probably adds value to electrodiagnostic studies in assessing carpal tunnel syndrome, as it can detect structural abnormalities (54). Twenty three articles were identified that potentially demonstrated the added value of neuromuscular ultrasound as a diagnostic tool when used in combination with electrodiagnostic studies, but only four of them were graded as Class II. Three of these articles described the

detection of bifid median nerves at the wrist, two studies described the detection of persistent median arteries, and one study also described the detection of tendosynovitis and accessory muscles within the wrist and occult ganglia causing median mononeuropathy. All 19 of the Class IV articles were case reports where HRUS was used to identify abnormal structures causing median mononeuropathy at the wrist. These structures included traumatic neuromas, schwannomas, fibrolipomatous hamartomas, ganglion cysts, thrombosed persistent median arteries, abscess, and compressive gouty tophus.

Concerning our case with *thrombosis of the persistent median artery* mimicking carpal tunnel syndrome, the diagnosis may be established easily by HRUS and/or MRI. Since 1958, only 17 cases of thrombosis of the persistent median artery as cause of a secondary carpal tunnel syndrome have been published. Females are most often affected with previous events such as trauma or repeated mechanical overload of the hand. The leading clinical symptom was acute brachialgia with pressure pain at the carpal tunnel without major sensomotor deficits of the median nerve. Results of systematic electrodiagnostic testing are lacking (78). A persistent median artery is quite often seen in asymptomatic normal individuals (up to 16%), its role in carpal tunnel syndrome however remains controversial (79-80). Another case report with congruent HRUS and MR-angiography findings was recently published (81). In the literature, resection of the median artery is recommended (81). We chose conservative treatment with ibuprofen and pregabalin as in another, unpublished case (personal communication from T. Schelle, Dessau), where spontaneous recovery of symptoms occurred within a period of several weeks or months. Cases of thrombosis of the median artery have been interpreted as secondary carpal tunnel syndromes. In a study, as electrodiagnostic testing of the median nerve was normal and no other pathology of the nerve was identified during surgery, the authors concluded that it probably represents not a secondary carpal tunnel syndrome but it constitutes an independent entity (58). Digital subtraction angiography is usually not necessary, because the tendency of the small arteries to spasms makes it difficult or even impossible (81).

In conclusion, in case of trauma or repetitive mechanical stress in the history with acute brachialgia and pain in the carpal tunnel one should think on this rare disease in the absence of signs of tendosynovitis and negative electrodiagnostic testing of the

median nerve. HRUS and 3T-MRI are suitable to establish the diagnosis. HRUS features include enlargement of the artery, which is non-compressible and without pulsation of the vessel wall, mostly with prestenotic resistance profile. The colour-fill in colour-duplex is not always present. The described new imaging methods will probably allow a better diagnostic accuracy.

Acute carpal tunnel syndrome after hyperventilation tetany have not been described until now. Independent of the site, nerves show the same morphologic changes under compression. In our case, the morphologic changes of the nerve with time were described. The sonographic compression signs (enlarged CSA and diameter, diminished echotexture and hypoechogenity) resolved spontaneously after 6 weeks and pathologic electrophysiological results after as little as within weeks.

Among different types of benign soft tissue tumours, only 10% originate from the peripheral nerve structure. They are also referred to as benign tumours of the peripheral nerve sheath. The most common types are *schwannoma* (synonym: neurinoma) and neurofibroma (69). Usually, a solid schwannoma affects a single fascicle only, whereas a solid neurofibroma arises from a fascicle group, which explains why schwannomas are easier to treat surgically. Both mass lesions are characterized by a slow growth over years or decades. Therefore, neurological abnormalities appear very late. Unfortunately, electrodiagnostic testing is of less value in the diagnosis because it can not reveal the pathology. In the two case reports with schwannoma, the correct localization of the lesion was provided only by HRUS. Schwannomas located proximally and distally from the carpal tunnel may mimic carpal tunnel syndrome in rare cases. In our case of the schwannoma at the wrist, progression was slow over 10 years. Interestingly, in this patient more than 50 years earlier a nerve injury occurred with some mild signs of median nerve lesion at the same level as the site of the schwannoma. Neuromas after severe nerve lesions are common, but very rarely even a schwannoma (neurinoma) can develop many years after a nerve lesion. This case seems to support this observation.

5.2.4. THORACIC OUTLET SYNDROME (TOS)

Our case with *TOS* is one of 4 unpublished cases from three neurologists (Thomas Schelle/Dessau, Steve Dettmann/Chemnitz and Josef Böhm/Freiberg), where HRUS indicates that the fibrous medial edge of the scalene medius muscle was the cause of neurogenic TOS. 3-Tesla MRI was also performed 3 of the 4 cases. Diagnosis was confirmed during surgery in all four cases. This anomaly has not been described before in the classification of fibromuscular band variants by Roos (82) and HRUS findings are not reported in the literature. In all four cases, patients were female and the symptoms presented on the right side. In one patient the left side was also subclinically affected. Pain was the predominant symptom only in one patient, paresis and atrophy of the small hand muscles, most visible in APB followed by ADM and interosseous muscles were more characteristic. Sensory deficits were found mostly in ulnar innervated area and only partly in the C8/Th1 dermatome. Definitive diagnosis was reached in 1-15 years. EMG showed in all cases chronic neurogenic changes in the C8 innervated muscles. F-wave-latency was abnormal in 3 cases. Motor neurography of the ulnar/median nerve was abnormal in 3 cases. Surprisingly, the sensory nerve action potential of the medial antebrachii cutaneous nerve, which was supposed to be a highly reliable test in TOS, was abnormal in only in 2 cases, as opposed to a study in this subject (83). Conventional X-ray images of the cervical spine and CT are of little diagnostic value. In 3 cases, cervical rib/rib stub with band attachment /enlarged transverse process of C7 was described. Only special sequences of 3 T-MRI (T1/STIR/PDW) with corresponding narrowing of the examined region are of limited informative value, and the resolution is inferior compared to HRUS. The “wedge/sickle-sign” with hyperechoic tip of the medial border of the medial scalene was consistent and was reproducible on four different ultrasound devices (Siemens, Toshiba, Philips, Mindray) with 3 different examiners. HRUS seems to be superior to conventional 3T-MRN. In 2 patients, follow-up has shown a clear clinical improvement, in the other 2 patients follow–up examination are pending.

The following drawing *(Fig. 29)* shows the anatomical relationship of the medial fibrous edge of the scalenus medius muscle to the inferior trunk of the brachial plexus in normal (left) subjects and in a pathologic (right) case causing TOS.

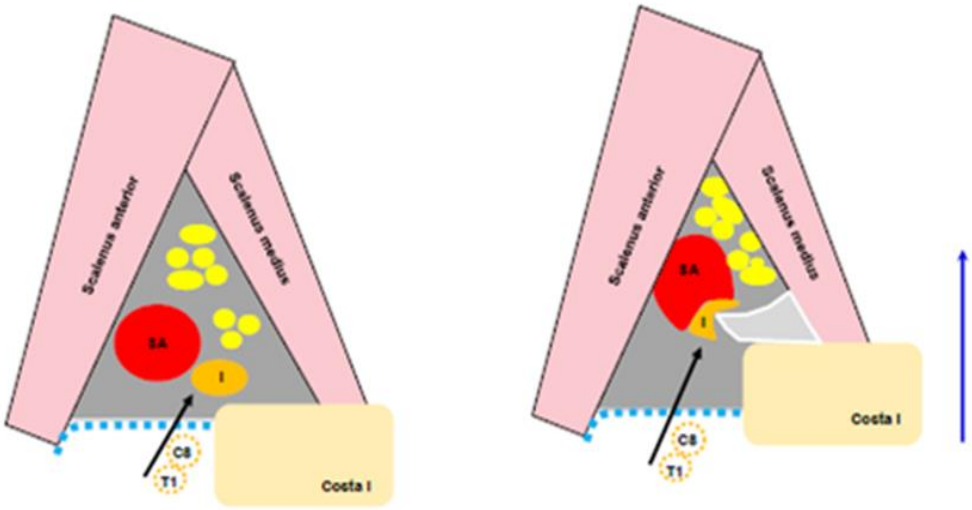

Fig. 29. Anatomical relationship in TOS caused by the fibrous edge of the median scalenus muscle. The truncus inferior (I) near the subclavian artery (SA) in its course in the triangle formed by the scalenus anterior and medius muscles and the first rib in normal subjects (left) and in TOS caused by compression of the inferior trunk by the edge of the scalenus medius muscle (coloured in grey, on the right). Thomas Schelle (Department of Neurology, Dessau-Roßlau /Germany).

5.2.5. NEURALGIC AMYOTROPHY (PARSONAGE-TURNER SYNDROME, PTS)

Among the different disorders of the brachial plexus, *"neuralgic amyotrophy"* was first described in detail by Parsonage and Turner (PTS) in 1957 (84). Aetiology of the idiopathic form is unknown so far. Several mechanisms, especially of autoimmune origin have been discussed (85). Comparable to motor neuron diseases, the incidence of 2–3/100.000 individuals/year regarding the idiopathic form is rather low (86).

In a smaller subgroup of patients, neuralgic amyotrophy may predominantly involve the anterior interosseous nerve or the radial nerve, as well as the lower brachial plexus. This applies particularly to women (87). Here, the typical clinical course of sudden onset helps to differentiate neuralgic amyotrophy from true focal compressive neuropathies. In 6% of cases, by means of MR imaging, a T2 lesion or hypertrophy of the brachial plexus has been described (90). There are no actual reports about ultrasound

imaging regarding Parsonage-Turner syndrome (PTS). According to my own experience, hypoechoic and long-segmental CSA enlargement of the affected roots, of parts of the brachial plexus, of peripheral nerves, or of even single fascicles can be detected, weeks after onset of the disease, but not at the beginning and not in all cases. As mentioned before, rare tumours and focal tumour-like lesions may be difficult to differentiate, e.g. it is extremely challenging to differentiate between a plexiform growing tumour and a focal manifestation of PTS. These focal lesions of completely different origin may present as a focal fusiform enlargement of the nerve and a hypertrophic-hypoechoic remodelling of its fascicles. In our first case on PTS with a predominant radial nerve palsy, HRUS showed segmental enlargement of the radial nerve distal to the spiral groove in the distal part of the upper arm only 3 months after onset. PTS may also cause bilateral palsy of the anterior interosseous nerve (AIN), as described in our second case. Similarly to AIN palsies in torsion neuropathy (72), the pathologic findings were not at the expected anatomical site distal from the elbow, but occurred in the median nerve within an approximately 9 cm section proximal to the medial epicondyle. This region corresponds to the area where dissection of nerve fascicles is anatomically possible. Further studies with large numbers of patients are needed to describe the morphologic changes in PTS and the sensitivity and specificity of HRUS in this disease.

5.2.6. RARE POLYNEUROPATHIES

HRUS may provide important morphologic information, which leads to the diagnosis of certain *rare polyneuropathies*. In our first polyneuropathy case, the role of HRUS was remarkable for the finding of long-segment enlargement of the ulnar nerve at a non-entrapment site caused by paraneoplastic neuropathy. Paraneoplastic neurological syndromes are well known to affect the peripheral nervous system and usually precede the diagnosis of a tumour by several months or years. The range of manifestations in the PNS is broad and includes acute inflammatory demyelinating neuropathy, distal symmetric axonal neuropathy, motor neuropathy, motor neuronopathy, sensory neuropathy, and sensory neuronopathy (88). The most common manifestation of patients with detectable anti-Hu antibodies in the PNS is painful axonal

preferentially sensory neuropathy or neuronopathy that predominantly affects the lower extremities (89). In contrast, multiple mononeuropathy is most often seen in vasculitides and connective tissue disorders. Nevertheless, it has also been observed in paraneoplastic neuropathies, but are distinctively rare (90). In this case, HRUS was especially useful in electrophysiologically severe, non-localizing axonal neuropathies (left-sided ulnar nerve in this case), by detecting multifocal nerve enlargement at non-entrapment sites. This case therefore vividly illustrates the added value of nerve ultrasound in the diagnostic work-up of suspected inflammatory or uncommon neuropathies in addition to electrophysiological studies and highlights an unusual but important paraneoplastic differential diagnosis of progressive multifocal hypertrophic neuropathies.

In our second case with *MADSAM neuropathy*, HRUS helped in localizing the pathological nerve segment at a site inaccessible to electric stimulation. As reported before (91), a remarkable finding was the detection of focal enlargement and change of echostructure of the nerve. The focal pathologic findings on peripheral nerves in HRUS are also seen on nerves that have functionally recovered after treatment. Ultrasound may also contribute to the differential diagnosis of acquired demyelinating neuropathies vs. motor neuron disease and further studies with larger patient numbers are required.

In our third case with distal-symmetric axonal *vasculitic neuropathy,* HRUS showed significantly larger tibial nerves at the ankle than in control subjects from a previous Japanese study (92). High-frequency sonography helped in two cases of multiple mononeuropathies and two cases of distal-symmetric polyneuropathy to reach the diagnosis of vasculitic neuropathy and was able to detect focal morphologic lesions, which could not be identified electrophysiologically due to the axonopathy. The tibial nerve at the ankle was always involved, but additional enlargement of nerves on the upper arm and/or brachial plexus was seen only in the multiple mononeuropathy type (93).

Due to the increasing importance of HRUS in the diagnosis of rare polyneuropathies, we retrospectively analysed the ultrasonographic findings in patients with multiple mononeuropathy of autoimmune origin in order to provide a preliminary summary on findings in this group of patients (unpublished results, under submission). Following clinical and electrophysiological assessment, 11 untreated patients with

dysimmune multiple mononeuropathy underwent ultrasonography of multiple upper and lower limb nerves. According to clinical diagnoses, groups of patients with multifocal motor neuropathy (MMN) (3 patients), multifocal acquired demyelinating sensory and motor neuropathy (MADSAM) (5 patients) and multiple mononeuropathy associated with other immunological disorders (1 patient with monoclonal gammopathy of uncertain significance [MGUS], 1 patient with systemic vasculitis, and 1 patient with multiple neuropathy of paraneoplastic origin) were formed. All patients demonstrated multiple segmental nerve enlargements and / or abnormal nerve echostructure, such as enlarged-fused fascicles, complete loss of fascicular structure and hypoechogenicity, both at sites of clinical-electrophysiological abnormality and at unaffected sites and nerves. Abnormalities preferentially occurred or were more marked at proximal nerve segments. No consistent pattern emerged that would enable to differentiate between dysimmune multiple mononeuropathies of different origin. We concluded that the routine use of HRUS as a complementary diagnostic tool in the work-up of these patients is very reasonable.

6. CONCLUSIONS AND FURTHER DIRECTIONS

In the first part of the thesis, we presented the results of our HRUS nerve measurements on healthy persons on the upper and lower extremities and the cervical roots aiming to gain information about cross-section normal values. We pointed out that among other studies our study is the first to evaluate most of the important nerves on the upper and lower limbs in the same person, including pure sensory nerves and cervical roots in a healthy Central-European population. There was a good correlation of our results with previous reports with only few nerve segment measurements and with recently published larger studies with similar nerve segment measurements. In order to use these reference values with confidence in everyday practice, we examined the reliability of these normal values, i.e. the congruence of values obtained by different examiners, ultrasound devices and by the same examiner at different time points. The intra-rater, interrater and inter-equipment reliability was high and we concluded that good reliability and reproducibility of our measurements serves as a basis for the acceptance of the normal values provided by our study. We pointed out, that predefined anatomical landmarks are essential to obtain comparable data.

In the second part, we discussed the clinical utility of HRUS in rare neuropathies of different aetiologies. Findings in rare tumours and focal tumour-like lesions, nerve torsion, rare diseases mimicking carpal tunnel syndrome, thoracic outlet syndrome, Parsonage-Turner syndrome and some rare polyneuropathies were described. It was concluded that findings of clinical examination, electrodiagnostic tests and MRI may be insufficient in clarifying the cause of certain rare neuropathies. HRUS provides useful additional information with regard to the region, extent and often the aetiology of the disorder, and it should be considered in the diagnostic work-up of patients with suspected rare neuropathy. HRUS shows typical morphological changes for individual clinical entities which can be effectively used in the differential diagnosis of peripheral nerve diseases. Presently, it is unclear whether new techniques such as ultrasound contrast agents, elastometric measurements and systematic analysis of nerve vascularisation will provide additional useful information to increase the diagnostic power of this method.

7. SUMMARY

High-resolution ultrasound (HRUS), introduced for peripheral nerve examination by Fornage in 1988, is a method that allows non-invasive imaging of numerous peripheral nerves with excellent image quality with high spatial resolution and can be modified and tailored immediately to the pathology seen by the examiner.

Using HRUS, we established reference values in healthy subjects for the most frequently examined nerve segments on the upper and lower extremities and for the cervical roots and assessed different aspects of reliability. Three objectives were examined. As a first step, we established a set of normal CSA values for C5, C6, and C7 cervical roots, and several upper and lower limb nerves, including some pure sensory nerves, at pre-defined anatomical sites, and assessed whether CSAs correlated with age, gender, height, and body weight. Second, we systematically assessed the reliability of these measurements on several nerves in the upper and lower limbs, with respect to intra-rater, inter-rater and inter-equipment variation. CSA values of two independent cohorts from the two study sites were also compared in order to determine the external validity of collected normal values. Thirdly, we analysed cases of rare neuropathies assessed by ultrasonography in order to establish the role of HRUS in rare disorders of the peripheral nerves.

Based on our results, the following conclusions are drawn:

1. The mean CSA of the 14 nerve segments ranged from 2 to 10 mm^2 and there was a good correlation of these results with previously reported normal values.

2. We found no consistent correlations between CSA values and age, height, or body weight, but males had significantly larger values than females for nerve segments in the upper arm.

3. The intra-rater, inter-rater and inter-equipment reliability was high with intraclass correlation coefficients of 0.93, 0.98, and 0.86, respectively.

4. HRUS shows typical morphological changes in certain rare neuropathies, which can be effectively used in the differential diagnosis of peripheral nerve diseases.

5. Findings of clinical examination, electrodiagnostic tests and MRI are often insufficient in clarifying the cause of rare neuropathies. HRUS in these cases provides useful additional information with regard to the region, extent and often the aetiology of the disorder.

8. ÖSSZEFOGLALÁS

A magas felbontású ultrahang, amelyet Fornage a perifériás idegek vizsgálatára először 1988-ban alkalmazott, számos perifériás ideg nem-invazív vizsgálatát teszi lehetővé, kiváló képminőséggel, magas axiális felbontással és gyors optimális kép fókuszálással a kóros folyamatra.

Ultrahangos vizsgálattal egészséges alanyoknál több felső és alsó végtagi ideg, valamint a nyaki ideggyökök keresztmetszetének területét mértük meg, valamint a mérések megbízhatóságának (reprodukálhatóságának, reliabilitásának) különböző szempontját is megvizsgáltuk. A tanulmány három célja közül elsőként a C5-ös, C6-os és C7-es ideggyök és több felső és alsó végtagi ideg keresztmetszeti területét mértük meg előre meghatározott anatómiai pontok magasságában, és megvizsgáltuk a keresztmetszeti terület összefüggését a korral, a nemmel, a testmagassággal és a testsúllyal. Ezt követően a mérések megbízhatóságának különböző aspektusait (ún. intra-rater, inter-rater és inter-equipment reliability) vizsgáltuk meg. A keresztmetszeti területi mérések két különböző népességben történtek (magyar és német) és az értékeket összehasonlítottuk. Harmadikként az ultrahang jelentőségét vizsgáltuk a peripheriás idegek különböző ritka kórfolyamataiban.

Eredményeink alapján a következő következtetéseket vontuk le:

1. A megvizsgált idegek keresztmetszete 2-10 mm² között volt és ezek hasonlóak voltak a korábban közölt tanulmányok értékeivel.
2. Nem találtunk összefüggést a keresztmetszeti terület és a kor, nem, magasság és testsúly között, csak a felkaron voltak a férfiak értékei nagyobbak, mint a nőké.
3. Az ún. intra-rater, inter-rater és inter-equipment reliabiliy magas volt, a csoportok közötti korrelációs koefficiensek 0,93, 0,98 és 0,86 voltak.
4. A magas felbontású ultrahang kimutatja az idegek jellegzetes morfológiai elváltozását ritka kórfolyamatokban és ezáltal jelentősen segíthet a peripheriás idegek betegségeinek differenciáldiagnózisában.
5. A peripheriás idegek kórfolyamataiban a klinikai leletek és az elektrofiziológiai, ill. mágneses rezonanciás tomográfiás (MRT) vizsgálatok eredményei sokszor nem elegendőek a ritka kórfolyamatok okának kiderítéséhez. Ilyen esetekben az ultrahang értékes információkat nyújt a peripheriás kórfolyamatok pontos helyéről, kiterjedéséről és gyakran okáról is.

9. REFERENCES

1. Rechtien JJ, Gelblum JB, Haig AJ, Gitter AJ. (1999) Guidelines in Electrodiagnostic Medicine. American Association of Electrodiagnostic Medicine. Muscle Nerve, 8(Suppl): S5-S12.
2. Padua L, Liotta G, Di Pasquale A, Granata G, Pazzaglia C, Caliandro P, Martinoli C. (2012) Contribution of ultrasound in the assessment of nerve diseases. Eur J Neurol, 19:47-54.
3. Koenig RW, Schmidt TE, Heinen CP, Wirtz CR, Kretschmer T, Antoniadis G, Pedro MT. (2011) Intraoperative high-resolution ultrasound: a new technique in the management of peripheral nerve disorders. J Neurosurg, 114:514-521.
4. Zaidman C, Seelig M, Baker J, Mackinnon S, Pestronk A. (2013) Detection of peripheral nerve pathology Comparison of ultrasound and MRI. Neurology, 80:1634-1640.
5. Solbiati L, De Pra L, Ierace T, Bellotti E, Derchi LE. (1985) High-resolution sonography of the recurrent laryngeal nerve: anatomic and pathologic considerations. AJR Am J Roentgenol, 145:989-993.
6. Fornage BD. (1988) Peripheral nerves of the extremities: imaging with US. Radiology, 167:179–182.
7. Kele H. (2012) Ultrasonography of the peripheral nervous system. Perspectives in Medicine, 1:417–421.
8. Padua L, Hobson-Webb L**. (**2013) Ultrasound as the first choice for peripheral nerve imaging? Neurology, 80:1626-1627.
9. Peer S, Gruber H. Atlas of Peripheral Nerve Ultrasound , Springer-Verlag, Berlin Heidelberg, 2013: 3-4.
10. Beekman R. High-resolution sonography of the peripheral nervous system. Thesis, Utrecht University, 2004 , Page 21, ISBN 90-393-3856-6
11. Liu F, Zhu J, Wei M, Bao Y, Hu B. (2012) Preliminary evaluation of the sural nerve using 22-MHz ultrasound: a new approach for evaluation of diabetic cutaneous neuropathy. PLoS One, 7(4):e32730.doi: 10.1371/journal.pone.0032730.

12. Bleve M, Capra P, Pavanetto F, Perugini P. (2012) Ultrasound and 3D Skin Imaging: Methods to Evaluate Efficacy of Striae Distensae Treatment. Dermatol Res Pract, 673706. doi:10.1155/2012/673706.
13. Kopf H, Loizides A, Mostbeck GH, Gruber H. (2011) Diagnostic sonography of peripheral nerves: indications, examination technique and pathological findings. Ultraschall Med, 32:242-263.
14. Gruber H, Peer S, Gruber L, Loescher W, Bauer T, Loizides A.(2014) Ultrasound imaging of the axillary nerve and its role in the diagnosis of traumatic impairment. Ultraschall Med. Mar 19. DOI: 10.1055/s-0034-1366089 [Epub ahead of print].
15. Silvestri E, Martinoli C, Derchi LE, Bertolotto M, Chiaramondia M, Rosenberg I. (1995) Echotexture of peripheral nerves: correlation between US and histologic findings and criteria to differentiate tendons. Radiology, 197: 291–296.
16. Hobson-Webb LD, Massey JM, Juel VC , Sanders DB. (2008) The ultrasonographic wrist-to-forearm median nerve area ratio in carpal tunnel syndrome. Clin Neurophysiol, 119:1353-1357.
17. Gruber H, Glodny B, Peer S. (2010) The validity of ultrasonographic assessment in cubital tunnel syndrome: the value of a cubital-to-humeral nerve area ratio (CHR) combined with morphologic features. Ultrasound Med Biol, 36:376-382.
18. Cartwright MS, Passmore LV, Yoon JS, Brown ME, Caress JB, Walker FO. (2008) Cross-sectional area reference values for nerve ultrasonography. Muscle Nerve, 37:566–571.
19. Zaidman CM, Al-Lozi M, Pestronk A. (2009) Peripheral nerve size in normals and patients with polyneuropathy an ultrasound study. Muscle Nerve, 40:960-966.
20. Haun DW, Cho JC, Kettner NW. (2010) Normative cross-sectional area of the C5-C8 nerve roots using ultrasonography. Ultrasound Med Biol, 36:1422-1430.
21. Tagliafico A, Cadoni A, Fisci E, Bignotti B, Padua L, Martinoli, C. (2012) Reliability of side-to-side ultrasound cross-sectional area measurements of lower extremity nerves in healthy subjects. Muscle Nerve, 46:717–722.
22. Won SJ, Kim BJ, Park KS, Yoon JS, Choi H. (2013) Reference values for nerve ultrasonography in the upper extremity. Muscle Nerve, 47:864-871.
23. Cartwright MS, Hobson-Webb LD, Boon AJ, Alter KE, Hunt CH, Flores VH, Werner RA, Shook SJ, Thomas TD, Primack SJ, Walker FO. (2012) Evidence-

based guideline: neuromuscular ultrasound for the diagnosis of carpal tunnel syndrome. Muscle Nerve, 46:287-293.

24. Pompe SM, Beekman R. (2013) Which ultrasonographic measure has the upper hand in ulnar neuropathy at the elbow? Clin Neurophysiol, 124:190-196.
25. Bayrak AO, Bayrak IK, Turker H, Elmali M, Nural MS. (2010) Ultrasonography in patients with ulnar neuropathy at the elbow: comparison of cross-sectional area and swelling ratio with electrophysiological severity. Muscle Nerve, 41:661-666.
26. Martinoli C, Bianchi S, Santacroce E, Pugliese F, Graif M, Derchi L. (2002) Brachial plexus sonography: technique for assessing the root level. Am J Roentgenol, 179:699-702 .
27. Peer S, Bodner G. High-Resolution Sonography of the Peripheral Nervous System, 2nd Revised Edition, Springer, Berlin Heidelberg, 2008.
28. Visser LH.(2009) High resolution sonography of the superficial radial nerve with two case reports. Muscle Nerve, 39:392-395.
29. Vispo Seara JL, Krimmer H, Lanz U. (1994) Monofasziculäre Nervenrotation. Handchir Plast Chir, 26:190-193.
30. Guerra WK, Schroeder HW. (2011) Peripheral nerve palsy by torsional nerve injury. Neurosurgery, 68:1018-1024.
31. Böhm J. (2010) Akut carpalis alagút szindróma hyperventilatio okozta tetania következtében. Magyar Radiológia, 84:1-4.
33. Kerasnoudis A, Pitarokoili K, Behrendt V, Gold R, Yoon MS. (2013) Cross sectional area reference values for sonography of peripheral nerves and brachial plexus. Clin Neurophysiol, 124:1881-1888.
34. Heinemeyer O, Reimers CD.(1999) Ultrasound of radial, ulnar, median and sciatic nerves in healthy subjects and patients with hereditary motor and sensory neuropathies. Ultrasound Med Biol, 25:481-485.
35. Won SJ, Kim BJ, Park KS, Kim SH, Yoon JS. (2012) Measurement of cross-sectional area of cervical roots and brachial plexus trunks. Muscle Nerve, 46:711–716.
36. Sugimoto T, Ochi K, Hosomi N, Mukai T, Ueno H, Takahashi T, Ohtsuki T, Kohriyama T, Matsumoto M. (2013) Ultrasonographic reference sizes of the

median and ulnar nerves and the cervical nerve roots in healthy Japanese adults. Ultrasound Med Biol, 39:1560-1570.

37. Foxall Gl, Skinner D, Hardman JG, Bedforth NM. (2007) Ultrasound anatomy of the radial nerve in the distal upper arm. Reg Anest Pain Med, 32:217-220.

38. Fryback DG, Thornbury JR. (1991) The efficacy of diagnostic imaging. Med Decis Making, 11:88–94.

39. Impink BG, Gagnon D, Collinger JL, Boninger ML. (2010) Repeatability of ultrasonographic median nerve measures. Muscle Nerve, 41:767-773.

40. Kluge S, Kreutziger J, Hennecke B, Vögelin E. (2010) Inter- and intraobserver reliability of predefined diagnostic levels in high-resolution sonography of the carpal tunnel syndrome - a validation study on healthy volunteers. Ultraschall Med, 31:43-47.

41. Hobbson-Webb LD, Padua L. (2009) Median nerve ultrasonography in carpal tunnel syndrome: findings from two laboratories. Muscle Nerve, 40**:**94–97.

42. Bäuerle J, Lochner P, Kaps M, Nedelmann M. (2012) Intra- and interobsever reliability of sonographic assessment of the optic nerve sheath diameter in healthy adults, 22:42-45.

43. Ballantyne SA, O'Neill G, Hamilton R, Hollman AS. (2002) Observer variation in the sonographic measurement of optic nerve sheath diameter in normal adults. Eur J Ultrasound, 15:145-149.

44. Shah S, Kimberly H, Marill K, Noble VE. (2009) Ultrasound techniques to measure the optic nerve sheath: is a specialized probe necessary? Med Sci Monit, 15:63-68.

45. Moretti R, Pizzi B, Cassini F, Vivaldi N. (2009) Reliability of optic nerve ultrasound for the evaluation of patients with spontaneous intracranial hemorrhage. Neurocrit Care, 11:406-410.

46. Rohr A, Riedel C, Reimann G, Alfke K, Hedderich J, Jansen O. (2008) [Pseudotumor cerebri: quantitative in-vivo measurements of markers of intracranial hypertension]. Rofo, 180:884-890.

47. Geeraerts T, Newcombe VF, Coles JP, Abate MG, Perkes IE, Hutchinson PJ, Outtrim JG, Chatfield DA, Menon DK. (2008) Use of T2-weighted magnetic resonance imaging of the optic nerve sheath to detect raised intracranial pressure. Crit Care, 12:R114. doi: 10.1186/cc7006.

48. Cartwright MS, Demar S, Griffin LP, Balakrishnan N, Harris JM, Walker FO. (2013) Validity and reliability of nerve and muscle ultrasound. Muscle Nerve, 47:515-521.
49. Padua L, Martinoli C, Pazzaglia C, Lucchetta M, Granata G, Erra C, Briani C. (2012) Intra- and internerve cross-sectional area variability: new ultrasound measures. Muscle Nerve, 45:730–733.
50. Kerasnoudis A, Klasing A, Behrendt V, Gold R, Yoon MS. (2013) Intra- and internerve crosssectional area variability: new ultrasound measures. Muscle Nerve, 47:146–147.
51. Penkert G, Böhm J, Schelle T. Focal Peripheral Neuropathies. Imaging, Neurological, and Neurosurgical Approaches. Springer-Verlag, Berlin Heidelberg, 2014.
52. Gennaro S, Fiaschi P, Pacetti M, Quarto E, Merciadri P. (2014) Extramedullary plasmacytoma of median and sural nerve. Neurol Sci, 35:487-488.
53. Dettmann S. (2013) Sekundäre Extramedulläre Plasmozytommanifestation am N. medianus: Ein seltener Befund in der hochauflösenden Nervensonografie (HRUS). Klin Neurophysiol, 44 - P161, DOI: 10.1055/s-0033-1337302.
54. Chin KY, Fessas C, Murison M. (2010) A case report and review of soft tissue metastatic squamous cell carcinoma of the upper limb in the absence of a primary tumour. J Plast Reconstr Aesthet Surg, 63:568-570.
55. Baker KR, Rice L. (2012) The amyloidoses: clinical features, diagnosis and treatment. Methodist Debakey Cardiovasc J, 8:3-7.
56. Pöschl P, Pels H, Schulte-Mattler W. (2013) Nervensonografie bei Amyloidneuropathie. Klin Neurophysiol, 44 - P162, DOI: 10.1055/s-0033-1337303.
57. Tracy J, Dyck P, Dyck J. (2010) Primary amyloidosis presenting as upper limb multiple mononeuropathies. Muscle Nerve, 41:710–715.
58. Wadhwa V, Thakkar RS, Maragakis N, Höke A, Sumner CJ, Lloyd TE, Carrino JA, Belzberg AJ, Chhabra A. (2012) Sciatic nerve tumor and tumor-like lesions - uncommon pathologies. Skeletal Radiol, 41:763-774.
59. Ladha SS, Dyck PJ, Spinner RJ, Perez DG, Zeldenrust SR, Amrami KK, Solomon A, Klein CJ. (2006) Isolated amyloidosis presenting with lumbosacral

radiculoplexopathy: description of two cases and pathogenic review. J Peripher Nerv Syst, 11:346-352.

60. Laeng RH, Altermatt HJ, Scheithauer BW, Zimmermann DR. (1998) Amyloidomas of the nervous system: a monoclonal B-cell disorder with monotypic amyloid light chain lambda amyloid production. Cancer, 82: 362-374.
61. Schweigert M. (2014) Ischiadicustumor steckte hinter progredienter Fussheberparese. Der Neurologe&Psychiater, 1557-59.
62. Gonzalvo A, McKenzie C, Harris M, Biggs M. (2010) Primary non-Hodgkin's lymphoma of the radial nerve: case report. Neurosurgery, 67:E872-E873.
63. Tsai WC, Chiou HJ, Chou YH, Wang HK, Chiou SY, Chang CY. (2008) Differentiation between schwannomas and neurofibromas in the extremities and superficial body: the role of high-resolution and colour Doppler ultrasonography. J Ultrasound Med, 27:161-166.
64. Pallis CA, Scott JT. (1965) Peripheral neuropathy in rheumatoid arthritis. Br Med J, 1(5443): 1141-1147.
65. Malipeddi A, Reddy VR, Kallarackal G. (2011) Posterior interosseous nerve palsy: an unusual complication of rheumatoid arthritis: case report and review of the literature. Semin Arthritis Rheum, 40:576-579.
66. Kransdorf, MJ. (1995) Benign soft-tissue tumors in a large referral population: distribution of specific diagnoses by age, sex and location. AJR, 164:395-402.
67. Abe T, Hoshiko M, Shinohara N, Takamatsu T. (1966) Isolated paralysis of the deep branch of the radial nerve thought to be the entrapment neuropathy. Rinsho Seikei Geka, 1:617-621.
68. Wilhelm A. (1970) Das Radialisirritationssyndrom. Handchirurgie, 2:139-142.
69. Yasunaga H, Shiroishi T, Ohta K, Matsunaga H, Ota Y. (2003) Fascicular torsion in the median nerve within the distal third of the upper arm: three cases of nontraumatic anterior interosseous nerve palsy. J Hand Surg Am, 28:206-211.
70. Guerra WK, Schroeder HW. (2011) Peripheral nerve palsy by torsional nerve injury. Neurosurgery, 68:1018-1024.
71. Hosi K, Ochiai N, Shinoda H. (1993) Median nerve paresis with hourglass deformed funiculi: a case report. Rinsho Useikeigeka, 28:1171-1174.

72. Nagano A, Shibata K, Tokimura H, Yamamoto S, Tajiri Y. (1996) Spontaneous anterior interosseous nerve palsy with hourglass-like fascicular constriction within the main trunk of the median nerve. J Hand Surg, 21A:266–270.

73. Lundborg G. (2003) Commentary: hourglass-like fascicular nerve compressions. J Hand Surg, 28:212-214.

74. Dellon AL, Mackinnon SE. (1987) Musculoaponeurotic variations along the course of the median nerve in the proximal forearm. J Hand Surg Br,12:359-363.

75. Qi HT, Wang XM, Li SY, Wang GB, Wang DH, Wang ZT, Zhang XD, Teng JB. (2013) The role of ultrasonography and MRI in patients with non-traumatic nerve fascicle torsion of the upper extremity. Clin Radiol, 68:479-483.

76. Rossey-Marec D, Simonet J, Beccari R, Michot C, Bencteux P, Dacher JN, Milliez PY, Thiebot J. (2004) Ultrasonographic appearence of Idiopathic Radial Nerve Constriction Proximal to the Elbow. J Ultrasound Med, 23:1003-1007.

77. Cartwright MS, Hobson-Webb LD, Boon AJ, Alter KE, Hunt CH, Flores VH, Werner RA, Shook SJ, Thomas TD, Primack SJ, Walker FO. (2012) Evidence-based guideline: neuromuscular ultrasound for the diagnosis of carpal tunnel syndrome. Muscle Nerve, 46:287-293.

78. Dutly-Guinand M, Müller M, Bleuler P, Steiger R. (2009) Karpaltunnelsyndrom auf Grund von einer Arteria mediana – Thrombose – Vier Fallbeispiele und Literaturzusammenfassung. Handchir Mikrochir Plast Chir, 41:179 –182.

79. Barbe M, Bradfield J, Donathan M, Elmaleh J. (2005) Coexistence of mulitple anomalies in the carpal tunnel . Clin Anat, 18:251 – 259.

80. D'Costa S, Narayana K, Narayan P, Jiji, Nayak SR, Madhan SJ. (2006) Occurrence and fate of palmar type of median artery. ANZ J Surg, 76 :484 – 487.

81. Schelle T, Lemke A, Pawlaczyk N , Schneider W. (2012) Die akut thrombosierte A. mediana. Sekundäres Karpaltunnelsyndrom oder eigenständiges Krankheitsbild? Klin Neurophysiol, 43:172-174.

82. Roos DB. (1976) Congenital anomalies associated with thoracic outlet syndrome. Anatomy, symptoms, diagnosis, and treatment. Am J Surg, 132:771-778.

83. Cakmur R, Idiman F, Akalin E, Genç A, Yener GG, Oztürk V. (1998) Dermatomal and mixed nerve somatosensory evoked potentials in the diagnosis of neurogenic thoracic outlet syndrome. Electroencephalogr Clin Neurophysiol, 108:423-434.

84. Parsonage M, Turner J. (1948) Neuralgic amyotrophy: the shoulder-girdle syndrome. Lancet, 1:973–978.

85. Suarez GA. Immune brachial plexus neuropathy. In: Dyck PJ, Thomas PK, editors. Peripheral neuropathy. Elsevier Saunders , Philadelphia, 2005:2299–2308.

86. MacDonald BK, Johnson AL, Goodridge DM, Cockerell OC, Sander JW, Shorvon SD. (2000) The incidence and lifetime prevalence of neurological disorders in a prospective community based study in the UK. Brain, 123:665–676.

87. van Alfen N, van Engelen BGM. (2006) The clinical spectrum of neuralgic amyotrophy in 246 cases. Brain, 129:438–450.

88. Rudnicki SA, Dalmau J. (2005) Paraneoplastic syndromes of the peripheral nerves. Curr Opin Neurol, 18:598–603.

89. Camdessanché JP, Antoine JC, Honnorat J, Vial C, Petiot P, Convers P, Michel D . (2002) Paraneoplastic peripheral neuropathy associated with anti-Hu antibodies. A clinical and electrophysiological study of 20 patients. Brain, 125:166–175.

90. Zivkovic SA, Ascherman D, Lacomis D. (2007) Vasculitic neuropathy—electrodiagnostic findings and association with malignancies. Acta Neurol Scand, 115:432–436.

91. Scheidl E, Böhm J, Simó M, Rózsa C, Bereznai B, Kovács T, Arányi Z. (2012) Ultrasonography of MADSAM neuropathy: focal nerve enlargements at sites of existing and resolved conduction blocks. Neuromuscul Disord, 22:627-631.

92. Ito T, Kijima M, Watanabe T, Sakuta M, Nishiyama K. (2007) Ultrasonography of the tibial nerve in vasculitic neuropathy. Muscle Nerve, 35:379-382.

93. Böhm J. (2009) A perifériás idegek vizsgálata nagy felbontású ultraszonográfiával vascularis neuropathiában. Ideggyogy Sz, 62:277-281.

10. PUBLICATIONS

10.1. Publications relating to the thesis

Böhm J, Scheidl E, Bereczki D, Schelle T, Arányi Z. (2014) High resolution ultrasonography of peripheral nerves: measurements on 14 nerve segments in 56 healthy subjects and reliability assessments. Ultraschall in der Medizin/European Journal of Ultrasound , DOI:10.1055/s-0033-1356385 IF: 4,116

Penkert G, Böhm J, Schelle T. Focal Peripheral Neuropathies. Imaging, Neurological, and Neurosurgical Approaches. Springer-Verlag, Berlin Heidelberg, 2014.ISBN 978-3-642-54779-9

Böhm J, Schelle T. (2013) Stellenwert der hochauflösenden Sonografie bei der Diagnostik peripherer Nervenerkrankungen. Akt Neurol, 40: 258-268. IF: 0,320

Böhm J, Scheidl E, Schelle T. (2013) Aktueller Stellenwert der HRUS bei der Diagnostik von Polyneuropathien. Neurotransmitter, 24:34-39.

Leypoldt F, Friese MA, Böhm J, Bäumer T. (2011) Multiple enlarged nerves on neurosonography: an unusual paraneoplastic case. Muscle Nerve, 43:756-758. IF: 2,367

Böhm J, Visser LH, Lehmann TN. (2011) High-resolution sonography of posttraumatic neuroma of the superficial radial nerve. Cent Eur Neurosurg, 72:158-160 IF: 0,838

Böhm J. (2010) Akut carpalis alagút szindróma hyperventilatio okozta tetania következtében. Magyar Radiológia, 84:1-4.

Böhm J. (2009) A perifériás idegek vizsgálata nagy felbontású ultraszonográfiával vascularis neuropathiában. Ideggyógyászati Szemle/Clinical Neuroscience, 62:277-281.

Böhm J. (2008) Az idegszonográfia alkalmazási területei. Bulletin of Medical Sciences / Orvostudományi Értesítő, 81:84-87.

Böhm J. (2008) A perifériás idegek vizsgálata nagy felbontású ultraszonográfiával. Magyar Radiológia, 82:280-286.

Hettler A, Böhm J, Pretzsch M, von Salis-Sogilo G. (2006) Piriformissyndrom infolge einer extragenitalen Endometriose. Nervenarzt, 77:474-477. IF: 0,711

Böhm J. (2003) Paraspastik, Polyneuropathie und „tumoröse Veränderungen" der Achillessehnen: Polyneuropathie als Begleitsymptom bei einer Systemerkrankung? Akt Neurol, 30:407-409. IF: 0.269

10.2. Other publications

Scheidl E, Böhm J, Simó M, Bereznai B, Bereczki D, Arányi Z. (2014) Different patterns of nerve enlargement in polyneuropathy subtypes as detected by ultrasonography. Ultrasound Med Biol, 40(6):1138-45. IF: 2,455

Scheidl E, Böhm J, Farbaky Z, Simó M, Bereczki D, Arányi Z. (2013) Ultrasonography of ulnar neuropathy at the elbow: Axonal involvement leads to greater nerve swelling than demyelinating nerve lesion. Clin Neurophysiol, 124:619-625. IF: 3,144

Scheidl E, Böhm J, Farbaky Z, Debreczeni R, Bereczki D, Arányi Z. (2013) A nagy felbontású ideg-ultrahang vizsgálatok jelentősége a perifériás idegek betegségeinek diagnosztikájában. Ideggyógyászati Szemle/ Clinical Neuroscience, 66:4-13. IF: 0,348

Scheidl E, Böhm J, Simó M, Rózsa C, Bereznai B, Kovács T, Arányi Z. (2012) Ultrasonography of MADSAM neuropathy: focal nerve enlargements at sites of existing and resolved conduction blocks. Neuromuscul Disord, 22:627-631. IF: 3,464

Schelle T, König R, Böhm J, Dettmann S, Gruber H. (2013) Sonografische Charakteristika von Raumforderungen peripherer Nerven. Neuro Transmitter, 24(11): 26.

Arányi Z, Böhm J. (2014) Unusual ultrosonographic findings after nerve trauma explained by Martin-Gruber anastomosis. Clin Neurophysiol. In press.

11. ACKNOWLEDGMENTS

I wish to thank **Dr. Henrich Kele** (Neurologist, Praxis Neuer Wall, Hamburg) , **Prof. Leo Visser** (St. Elisabeth Hospital Tilburg, Dept. of Neurology and Clinical neurophysiology, Tilburg, The Netherlands), **Prof. Dr. Sigfried Peer** and **PD Dr. Hannes Gruber** (Dept. of Radiology, University of Innsbruck, Austria). They introduced me to high–resolution sonography (HRUS). My special thanks go to Dr. Erika Scheidl (Dept. of Neurology, Semmelweis University in Budapest). All my experimental work with normal values and reliability assessments was done together with her. I wish to thank above all **Dr. Thomas Schelle** (Dept. of Neurology, Dessau-Roßlau, Germany) for his extensive knowledge, experience, continuing support and friendship. This thesis would have been impossible without the results of our joint research, especially in the field of rare neuropathies.

I wish to thank furthermore the German neurosurgeons **Dr. Thomas-Nicolas Lehmann** (Dept. of Neurosurgery, Bad Saarow) and **Prof. Dr. Götz Penkert** (Praxis for Neurosurgery, Hannover) for widening my knowledge on neurosurgical aspects of peripheral nerve diseases.

I wish to thank all volunteers in Budapest and Freiberg who participated on the sonographic examinations to establish normal values.

I wish to thank my consultant **Prof. Dr. Dániel Bereczki**, Head of the Dept. of Neurology, Semmelweis University in Budapest and also **Dr. Zsuzsanna Arányi**, and all of the colleagues in Budapest for their valuable help and support, making my study stay in Budapest possible, where the experimental part of my work was performed.

I wish to thank my family for being there for me.